AN ABSTRACT OF THE THESIS OF

Benjamin A. Flugstad for the degree of Master of Science in Bioresource Engineering presented on January 12, 1996. Title: A Predictive Model for Time Domain Reflectometry Soil Water Content and Salinity Measurements.

Redacted for Privacy

Abstract approved: _____
John S. Selker

Redacted for Privacy

_____
Marshall J. English

Soil water content and water potential are two important parameters in determining the status of water in the soil. Improvement in the ability to measure these parameters by way of increased speed, accuracy, resolution, imaging volume, ease of automation, as well as reduced calibration requirements and reduced soil disturbance would be of utility to many applications in agriculture and engineering. To make the measurements economically and without the use of hazardous materials or methods would also be of value. A brief review is given on most of the existing water content and water potential measurement techniques with focus given on electromagnetic and quantum mechanic techniques due to their potential for best balancing the design goals. A review of the theories of electromagnetics and quantum mechanics are presented with applications to soil water content and water potential measurements. One electromagnetic method, Time Domain Reflectometry, or TDR, shows great promise in balancing all the desired design goals. A mathematical model is proposed to be able to predict TDR water content and electrical conductivity (or salinity) measurement results over wide ranges of those parameters. Preliminary validations were performed on the model for both invasive and potentially non-invasive TDR probes in a sandy soil with the results showing good agreement between predictions and actual results but with some model refinements still needed. A proposal for ongoing research is given to refine the models and address the question on the feasibility of using the models in a field grade TDR instrument to measure water content and electrical conductivity (or salinity).

**A Predictive Model for Time Domain Reflectometry
Soil Water Content and Salinity Measurements**

by

Benjamin A. Flugstad

A THESIS

submitted to

Oregon State University

in partial fulfillment of
the requirements for the
degree of

Master of Science

Presented January 12, 1996
Commencement June 1996

Master of Science thesis of <u>Benjamin A. Flugstad</u> presented on <u>January 12, 1996</u>

APPROVED:

Redacted for Privacy

Co-Major Professor, representing Bioresource Engineering

Redacted for Privacy

Co-Major Professor, representing Bioresource Engineering

Redacted for Privacy

Head of Department of Bioresource Engineering

Redacted for Privacy

Dean of Graduate School

I understand that my thesis will become part of the permanent collection of Oregon State University libraries. My signature below authorizes release of my thesis to any reader upon request.

Redacted for Privacy

Benjamin A. Flugstad, Author

TABLE OF CONTENTS

TABLE OF CONTENTS (Continued)

LIST OF FIGURES

LIST OF FIGURES (Continued)

LIST OF TABLES

A Predictive Model for Time Domain Reflectometry Soil Water Content and Salinity Measurements

1. INTRODUCTION

In recent years the need for water conservation has become more urgent due to the conflicting demands on water by an increasing population, agricultural users, as well as recreational and environmental advocates. This necessitates the need for more comprehensive monitoring of the fate of water in various systems such as in the soil, atmosphere, living biomass (plants & animals) and surface fresh water bodies (lakes and rivers). This thesis concentrates on methods for monitoring the fate of water in the soil.

A number of different soil properties are important in the modeling and/or characterization of a particular soil. Among these are bulk density, porosity, particle size distribution and saturated hydraulic conductivity. These are often assumed constant (neglecting seasonal compaction) over time and can therefore be measured or determined at infrequent intervals without much loss in accuracy. This allows use of invasive or destructive methods as well as slower methods to collect the information for these parameters without sacrificing decision making.

On the other hand, soil water content (on a volume or mass basis), water potential (matric + gravitational) and unsaturated hydraulic conductivity are variables with time and therefore need to be measured more frequently. Unsaturated conductivity can be determined using tension infiltrometers and other methods with discussion left to other authors. This thesis will discuss soil water content and water potential measurement techniques with emphasis on minimum-disturbance, fast and automated techniques such as electromagnetic and quantum mechanic methods.

Traditional methods of soil water content measurements such as gravimetric are both slow (overnight oven drying) and result in disturbance to the soil (especially when numerous samples are taken). More modern techniques such as Time Domain Reflectometry (TDR) and Neutron Probes have improved greatly on the speed of measurement problem and have reduced somewhat the soil disturbance problems by utilizing permanent access tubes or removable probes. These methods, however, in their present implementation, still present problems in that these permanent access tubes are not always desirable in various places such as agricultural fields where tractors have to maneuver around them. Also Neutron Probes have potential health risks as well as disposal problems due to their radioactivity. Soil water potential measurement techniques are also largely invasive and utilize mainly vacuum pressure sensors (tensiometers) and electrical resistance sensors (Water Mark sensors and gypsum blocks).

If automated data acquisition is needed then the equipment must be left in the ground and dataloggers or telemetry systems must be interconnected to these sensors. Again having sensors permanently in the ground creates problems for farmers who must work around them with their farm equipment. This usually means that only small restricted areas of farm fields will have access ports or sensors in them and therefore assumptions about the spatial variability and heterogeneity of the whole farm field must be made in order to extrapolate the data to make general conclusions. Cost considerations also limit the number of locations that the probes can be placed at on a field.

This therefore has created a need (or desire) for reduced-disturbance or non-invasive soil moisture measurement techniques which are also fast, automated, and accurate, have high resolution and wide imaging area, and are economical, convenient and portable. One electromagnetic technique, Time Domain Reflectometry, or TDR, shows great promise in balancing all these goals and so will be the focus of ongoing research proposed in this thesis.

An overview of most of the existing techniques to measure water content and water potential is presented. These methods are categorized as follows:

A.) Direct Methods (Gravimetric)

B.) Indirect Methods
    I.) Geophysical
        - Gravitational Variations
        - Pyschrometry (relative humidity)
        - Tensiometers
        - Piezometer Tube

    II.) Thermal
        - Heat Capacity (Thermal Capacitance)
        - Heat Dissipation (Thermal Resistance)

    III.) Radioactive
        - Neutron Probe
        - Gamma Ray Attenuation

    IV.) Electromagnetic
        a.) Electric Field Methods
            - Bulk Soil Resistance
            - Resistance of device in equilibrium with the soil
                i) Gypsum Blocks
                ii) Water Mark Sensors
            - Soil Capacitance
        b.) Magnetic Field
            - Induced Fields (Inductive)
            - Fluctuations in Earth's Magnetic Field
        c.) Electromagnetic Wave Propagation & Reflection
            - Time Domain Reflectometry (TDR)
            - Ground Penetrating Radar (GPR)
            - Microwave Remote Sensing (large scale)
            - Microwave Backscattering (small scale)
        d.) Quantum Mechanic (Nuclear Magnetic Resonance (NMR))

A brief discussion of all of these techniques is given with emphasis placed on the electromagnetic and quantum mechanic methods. Conclusions are given on which techniques offer the greatest potential in achieving or balancing the design goals of accuracy, automation, reduced soil disturbance, larger zone of influence, speed and ease of measurement, reduced calibration requirements, no hazardous materials, lower cost of measurement, and higher measurement convenience.

One promising technology (TDR) will be discussed in greater depth along with some of the potential problems it faces (accuracy when salinity is high) as well as a description of a mathematical model which may eliminate these problems. Preliminary experimental validations of this model were performed with some of those results given. More comprehensive model validations and refinements will occur as part of a proposed research project. A proposal for this ongoing research, which will investigate the feasibility of using this developed mathematical model (based on electromagnetic theory) for extending the usability of TDR, as an accurate soil water content and salinity or electrical conductivity measurement tool, into regions of high salinity over wide ranges of soil water content and soil types will be given. This ongoing research will be the subject of the author's Ph.D. work.

2. OVERVIEW OF SOIL MOISTURE MEASUREMENT TECHNIQUES

There are a number of different techniques to measure soil water content. These methods can be categorized into direct methods (methods which measure the desired parameter directly) and non-direct methods (methods which correlate water content and/or water potential to some other measurable parameter such as the soil dielectric constant (Topp et. al. 1980), or the soil heat capacity (Bristow et. al. 1993)).

One of the categories within indirect methods: electromagnetic methods, is divided into the following subcategories: Electric field techniques (soil dielectric constant and electrical conductivity or resistance), magnetic field techniques (soil magnetic permeability, diamagnetic, paramagnetic and ferromagnetic properties), electromagnetic wave techniques (variation in the phase velocity and attenuation of the waves due to the electric permittivity, magnetic permeability, electric conductivity, and resulting impedance of the soil), quantum mechanic techniques (Nuclear Magnetic Resonance (NMR)) as well as combinations of the above properties.

A number of comprehensive studies have already been conducted on soil moisture measurement techniques (Gardner, 1986; Klute, 1986; Phene et al., 1990; Jury et al., 1991; Topp et al., 1992)) and so concentration here is on the electromagnetic and quantum mechanic methods of determining water content and water potential with only a brief overview given on non-electromagnetic techniques.

2.1 Direct Methods of Measuring Soil Moisture

Direct methods involve measuring the desired parameter (water content) directly. The main example of a direct method for measuring water content is gravimetric analysis. Gravimetric methods involve taking a soil core from the field and weighing the sample while wet and then drying the sample for 24 hours in an oven dryer at some specific temperature (typically 105 degrees C) and then weighing the sample again while dry. The volumetric water content can then be obtained directly from the following formula:

$$\theta \; = \; \frac{\text{Volume of Water}}{\text{Soil Core Volume}} \; = \; \frac{(\text{Mass of Wet Soil - Mass of Dry Soil})}{(\text{Soil Core Volume})(1 \text{ g } H_2O \text{ / cc})} \quad (1)$$

This formula assumes that the density of water is approximately 1 g/cc. This method is the most direct method in obtaining volumetric water content and is often used as a calibration standard for other water content measurement techniques. It is also relatively simple to execute and relatively inexpensive.

There are three main disadvantages of the gravimetric method of determining water content. First, the soil is disturbed in that a soil core needs to be taken. Second, it takes 24 hours to get the water content result and third, there is no way to automate gravimetric water content measurements. These disadvantages led to the development of the indirect measurement techniques to be discussed next.

2.2 Indirect Methods of Measuring Soil Moisture

Water content, water potential and even just macroscopic locations of water or aquifers can often be obtained indirectly by correlating those parameters to some other readily measurable parameter. This section discusses many of these methods. Most of the methods deal with the measurement of volumetric water content or the location of macroscopic water aquifers in the subsurface media. A number of other methods measure the water potential or the amount of energy per unit weight of water (head in cm) or in other words a quantifier on the degree of difficulty in pulling water out of its present location.

2.2.1 Geophysical Methods

2.2.1.1 Gravitational Variations

Variations in the gravitational constant, g, can be used to detect significant density changes in the soil and subsurface media and thus detect locations of water. The gravitational constant is often found from the "Earth equation" given as follows (Milsom, 1989):

$$g = 9.780327 + 5.27904\text{E-}2\ \sin^2 L + 2.327\text{E-}4\ \sin^4 L \tag{2}$$

where L is the degrees in latitude and g is measured in units of m/s^2. This equation is a macroscopic equation based on averaged measurements of g at different points on the earth. The equation shows g is least at the equator and this is due to both the outward centrifugal force on objects at the equator due to the rotation of the earth as well as the fact that the equator is slightly further from the center of the earth than the poles are

(Halliday and Resnick, 1977). On a smaller scale there are variations from this equation due to localized density changes in the earth and these variations can be used to find water at different depths. This method can help locate density changes of the subsurface media at depths of 1 meter to 10's of kilometers depending on how far apart in distance g is measured at and compared to the above equation or how much it varies over a particular distance. This can help locate water or aquifers but it is difficult to determine exact water content at a particular depth with this method due to lack of discrimination between sources of density variations.

2.2.1.2 Seismic Methods

Seismic methods can be used to determine the elastic properties of soil as well as density changes at different depths in the soil with this information being used to determine where water is present. Two different types of waves can be propagated. One is a compression wave, which behaves like sound waves, and the other is a shear wave, which behaves like waves on the ocean surface. A bullet fired into the soil, the dropping of a weight, or an explosion with TNT can be used to trigger the waves depending on how much energy is required to probe the depth of interest. When the propagating wave hits a discontinuity in density and/or elastic properties (such as an aquifer boundary) it reflects at an angle opposite to its angle of incidence. For a normal incident wave the reflection coefficient is given by the following equation:

$$R_c = \frac{\rho_2 v_2 - \rho_1 v_1}{\rho_2 v_2 + \rho_1 v_1} \tag{3}$$

where ρ is the density of the materials (kg/cubic meter), v is the velocity of the wave (m/s), and the subscripts 1 and 2 indicate the values of these parameters before and after the density and/or elastic property discontinuity, respectively. The amount of wave that returns to the surface as well as the length of time it takes to return to the surface can help

indicate how much water is present and how deep it is. The degree of saturation effects the elastic properties of the soil due to the incompressibility of water and effects the density of the soil due to water replacing air in the soil. With present technology, exact determination of water content is difficult to achieve with this method, although it is useful for locating the position of the water table in many cases.

2.2.1.3 Pyschrometry (relative humidity)

This method is used to measure the water potential in the soil through a thermodynamic relationship to the measured relative humidity in the soil. The water potential of the water vapor phase can be determined from the following equation (Jury et al., 1991):

$$\text{Relative Humidity} = \frac{P_v}{P_v^*} = e^{M_w \psi_w / \rho_w RT} \tag{4}$$

where P_v = Vapor Pressure (bars or kPa)

P_v^* = Saturated Vapor Pressure (bars or kPa)

M_w = Molecular Weight of water (grams/mole)

ψ_w = Vapor Water Potential (equal to liquid water potential at equilibrium)(m).

ρ_w = Density of Water (kilograms/cubic-meter)

R = Universal Gas Constant (8.314 Joules/mole-degK)

T = Temperature (degrees Kelvin)

This method is attractive in that it only requires the insertion of a thermocouple into the soil sample, but it is invasive to the soil sample and only provides water potential rather than water content. The method is limited to tension ranges of 100 cm (0.1 bar) to 700 meters (70 bars), with considerable loss of accuracy at tensions < 1 bar (wetter soils).

2.2.1.4 Tensiometers

Another geophysical device that measures water potential is the tensiometer. It consists of a fixed volume column of water that is in equilibrium with the soil via a porous cup at the bottom of the column. Vacuum pressure or tension can be read at the top of the water column with a vacuum gauge to then indicate water potential. This method of measuring water potentials is limited to the tension ranges of 0 to 800 cm of tension before dissolved gases form bubbles in the liquid column. Although most of the commercial products make use of manual vacuum gauges, devices are available that are fitted with pressure transducers and interfaced to automated data acquisition systems and dataloggers. Advantages of these devices include relative simplicity of installation as well as the fact that they are relatively inexpensive.

The tensiometer has several disadvantages: The devices have to be left in the field so that they remain in equilibrium with the soil which can lead to problems if tractors have to maneuver around them. They respond slowly to changing field moisture which could be a problem. They become increasingly more difficult to install and use at greater soil depths and again, they are not suitable for use in dry conditions with tensions greater than 800 cm. They also require considerable maintenance, and are subject to frequent failure due to loss of soil contact and leaks.

2.2.1.5 Piezometer Tube

This method can be used to measure positive pressure water potentials (saturated soils, or water under pressure). It consists of a tube placed into the soil with a water entry point where the measurement is desired. The height of the water in the tube indicates pressure potential of the system at the water entry point. These are very useful in determination of local gradients in head, but not suitable for most water management decision making.

2.2.2 Thermal Methods

2.2.2.1 Heat Capacity (Thermal Capacitance)

The heat capacity of a soil (the ability of a soil to store heat) can be used as an indicator of the amount of water in the soil. The heat capacity of water is generally much higher than the soil solids and certainly higher than the air component. An equation to relate the heat capacity of the soil to the volumetric water content is shown as follows (Jury et al., 1991):

$$C_{\text{Soil}} = \theta + 0.46 \left(1 - \phi - X_0 \right) + 0.60 \, X_0 \tag{5}$$

Where C_{Soil} = Heat Capacity of the Soil Per Unit Volume $\left(\dfrac{\text{Cal}}{\text{cm}^3 \, {}^0\text{C}} \right)$

θ = Volumetric Water Content

ϕ = Porosity

X_0 = Volumetric Organic Matter Content

The heat capacity of the soil can then be measured directly by a calorimeter and the water content determined by the above equation. One disadvantage of this method is that organic fraction of the soil needs to be known as well as the porosity to be able to determine water content.

A variation of this method makes use of a heat-pulse probe to determine the volumetric specific heat of the soil from which volumetric water content can be determined (Bristow et al., 1993). They showed that volumetric water content can be determined from the following equation:

$$\theta = \frac{\dfrac{q}{\pi r_m^2 \Delta T_m e} - \rho_b c_m}{\rho_w c_w} \tag{6}$$

where q   =   Heat input to a line source in the probe (J/m)

ΔT_m =   Maximum temperature rise at a distance r_m from the probe.

ρ_b =   Soil bulk density $(\dfrac{kg}{m^3})$

ρ_w =   Density of water $(\dfrac{kg}{m^3})$

c_m =   Specific heat of the soil minerals $(\dfrac{J}{kg\ ^0K})$

c_w =   Specific heat of water $(\dfrac{J}{kg\ ^0K})$

They concluded that this heat-pulse method was very effective in determining water content when the probe spacings were known and well controlled (i.e. rigid needle probes) and when externally caused thermal gradients (e.g. mid-day heat) in the soil were either small or accounted for. This latter problem showed up near the surface of the soil and could be minimized by taking measurements early in the morning or late in the evening. Measuring background temperature was also considered by the authors as a possible way to account for excessive thermal gradients near the soil surface.

In general these heat capacity methods show promise as techniques for measuring water content if good thermal connections can be made to the soil, organic matter content is known, the effects of thermal gradients are accounted for and information about the soil porosity and soil bulk density are known. These methods are invasive and require considerable calibration in their present form. More research is needed on these methods.

2.2.2.2 Heat Dissipation (Thermal Conductivity)

As water content rises, the thermal conductivity of the soil rises rapidly due to the fact that the thermal conductivity of water is 20 times higher than that of air. Theoretically, regression equations could be developed to correlate water content and/or water potential to thermal conductivity. By supplying a heat source to a portion of soil one could measure the rise of temperature in the medium and obtain the thermal dissipation which is related to resistance and inversely related to thermal conductivity.

Commercial devices have been developed which measure water potentials from 10 to 300 meters tension using thermal resistance devices (Phene et al., 1990). These devices were shown to be accurate even in the presence of salinity and temperature changes in the soil and that information on the soil texture was not needed. The method was also shown to respond rapidly to changes in soil water potential.

The main disadvantage of thermal dissipation methods is maintaining a good thermal contact with the soil under test. Air gaps and other thermal insulating films will affect measurement accuracy. Also other variables such as soil compaction and the type of solids (e.g. thermally conductive metals) that are in the soil will also effect thermal conductivity and therefore measurement accuracy. This method is also invasive to the soil. More research is needed on this method to determine its suitability as a water content and/or water potential measurement technique.

2.2.3 Radioactive Methods

2.2.3.1 Neutron Probe

Water content can be measured by a method called neutron thermalization. A neutron probe is placed in an access tube in a soil and it emits "fast" (high energy) neutrons. The nuclei of hydrogen atoms (the majority of which are constituents of the water molecule) are efficient at deenergizing these neutrons. This process is called thermalization and the result is a number of "slow" or deenergized neutrons in proportion to the water content of the soil. These slow neutrons can be detected and statistically counted. Water content can then be estimated by an equation of the following form (Cuenca, 1989):

$$\theta = a_1 \left(\frac{NMC}{STD} \right) + b_1 \tag{7}$$

where NMC = neutron meter count (detected slow or thermalized neutrons)

STD   = standard count for the particular neutron probe

a_1, b_1 = statistical calibration coefficients

Advantages of this method are that it is quite precise if calibrated to the soil and that it can be used to rapidly determine water content to an arbitrary depth. In most soil conditions the neutron probe is an accurate method of measuring water content below the top 15 cm of soil.

The major disadvantage of the neutron probe is the fact that it involves radioactivity and requires special certification to operate. The device is also fairly expensive and requires a user (can't leave it in an automated test system or data acquisition system). The device requires lined access tubes for making the measurement.

Another disadvantage is that it has accuracy problems in the top 15 cm of soil due to neutrons escaping into the air. Cuenca et al. (1996) developed a quadratic regression equation to help account for the inaccuracies at shallow depths:

$$\theta = a_2 \left(\frac{NMC}{STD} \right)^2 + b_2 \left(\frac{NMC}{STD} \right) + c \qquad (8)$$

Other potential inaccuracies can occur if organic matter is very high creating another source of hydrogen atoms which can give the appearance of higher than actual water content. Finally other atoms in the soil such as Iron can absorb the slow or thermalized neutrons affecting the detected count.

2.2.3.2 Gamma Ray Attenuation

Gamma rays (wavelengths in the 5E-13m to 1.4E-10m range or frequencies in the 2E+18 to 6E+20 Hz range) are adsorbed in a predictable and repeatable manner with all the dry soil particles in a soil. Water added to the mix increases the gamma adsorption, which can be detected at the other end of a test column of soil, and used to estimate volumetric water content as long as the soil is a non-swelling soil (i.e. no smectite clay, etc.). A calibration equation of the following form can be used to relate the detected counts of gamma radiation to the volumetric water content (Jury et al., 1991, Gardner, 1986):

$$n(L) = n_0 \, e^{\left(-v_m \rho_b L - v_w \rho_w \theta_v L \right)} \qquad (9)$$

where $n(L)$ is the number of counts of gamma radiation per unit time at the detector and L is the thickness of the soil sample and v_w and v_m are the water and soil mineral gamma ray adsorption coefficients, respectively. In swelling soils where the bulk density of the solids changes with water content, or in cases where several fluids are present (e.g. oil), two

separate beams of different energies are employed to solve for all the unknowns and determine fluid content.

The advantages of this method include good precision as well as the ability to measure multiple fluid contents. The main disadvantage of this method is again the use of radiation with the requirements of lead shielding and specially designed collimators for safety. In addition, this method requires a transmission set-up, which is often impractical in field settings.

2.2.4   Electromagnetic Methods

The electromagnetic and quantum mechanic methods of measuring water content and/or water potential will be discussed only briefly here and then in more depth in the theoretical background section. These methods offer the greatest promise of balancing the design goals of reduced soil disturbance, good measurement accuracy and resolution, measurement speed, measurement automation and reduced measurement calibration in going from location to location. The theory of electromagnetics, quantum mechanics and Einstein's theory of relativity all are interrelated and serve as the basis for these measurement techniques and that background theory is reviewed in the discussion section.

2.2.4.1   Electric Field Techniques: Bulk Soil Resistance

The bulk resistance of the soil can give information about the amount of water in the ground or give information about where water is. This method assumes that the water in the soil contains mobile ions to make the water much more conductive and have much lower electrical resistance than the soil solids. By applying a known voltage between two electrodes or probes and measuring the current between them, the electrical resistance can be measured as given by Ohm's law shown in equation 10:

$$R = \frac{V}{I} \qquad (10)$$

where R is the electrical resistance in Ohms, V is the voltage between the electrodes in Volts and I is the current flowing from one electrode to the other in Amps. R can be related to the electrical conductivity σ by the following formula:

$$R = \frac{d}{\sigma A} \qquad (11)$$

where d is the distance between the electrodes and A is the cross sectional area of the electrodes and current path. The electrical conductivity can be related to the fraction of water filled pores by a variation of Archie's Law given as follows:

$$\sigma = \frac{\sigma_w \phi^{b} f^{c}}{a} \qquad (12)$$

where σ_w is the electrical conductivity of the soil water (S/m), ϕ is the porosity, f is the fraction of water filled pores and a, b and c are constants. More complicated equations can be developed for different types of probe or electrode arrangements where current might not flow uniformly through the earth (a likely scenario). These equations can be used to gain some information about how much water is in the soil as well as how deep it is by using different electrode spacings. Variations of this method can also be used to make determinations on the salinity or electrical conductivity of the soil. Often four-wire connections will be used to separately measure voltage and current for more accuracy.

The main advantage of this method is its simplicity. One of the major limitations of this method is the non-heterogeneity of the soil and how it can effect resistance measurements. Another limitation is any air gaps that might be in series with the current path.

2.2.4.2 Electric Field Techniques: Gypsum Blocks

Water Potential can be measured indirectly by placing a Gypsum block (Calcium Sulfate, $CaSO_4$) in the soil and letting it reach equilibrium with the soil water around it and then measuring the electrical resistance across it. A regression or calibration equation can then be used to relate water potential to the measured resistance across the block. This method is accurate in the 10m to 150m tension range but tends to get more nonlinear in the wetter ranges and therefore loses accuracy in those ranges.

An advantage of the device is that it is fairly insensitive to the effects of salinity in the soil although its electrodes can be fouled by salinity. Another advantage is that the method is relatively inexpensive and can be easily automated once the device is installed.

A disadvantage to this method is that the device disintegrates over time minimizing the measurement accuracy the longer it sits in the soil. Another disadvantage is the variability between blocks which can cause accuracy problems and increase calibration requirements. A major limitation to this device is that it must be buried in the soil medium (a large amount of soil disturbance) and good contact must be maintained to the adjacent soil matrix for accuracy. The sensor is also slow in responding to changing soil moisture.

2.2.4.3 Electric Field Techniques: Water Mark Sensors

This is a variation of the gypsum block and is useful in measuring water potential in the ranges of 100 cm to 2000 cm of tension (10 kPa to 200 kPa), (Wang et al., 1988; Thomson et al., 1987). The probe consists of a small cylindrical block of a medium similar to fine sand but containing a component of gypsum to minimize the effects of soil salinity. The electrical resistance is then measured across the device after it has reached equilibrium with the soil and a calibration curve is used to determine water potential. This device is

more accurate in these lower tension ranges than regular gypsum blocks but the absolute accuracy of these devices over time is still unclear due to degradation effects. They are less expensive than heat dissipation probes and require simpler electronics. One commercial product utilizing this method is manufactured by the Irrometer Company of Riverside, CA. The original device was invented by G.F. Larson in the late 1970's and patented in 1985 (Pogue, 1990).

2.2.4.4 Electric Field Techniques: Bulk Soil Capacitance

If a sample of soil is placed between two parallel plates of area A and separation d, then the capacitance (Farads) is given by the following formula:

$$C = \frac{\varepsilon\, A}{d} \tag{13}$$

where ε is the electric permittivity of the soil medium and is given as follows:

$$\varepsilon = \varepsilon_r \varepsilon_0 \tag{14}$$

where ε_r is the relative permittivity or dielectric constant and ε_0 is the permittivity of free space and is equal to 8.854E-12 Farads/Meter. Capacitance can be readily measured using a Schering Bridge, Wein Capacitance bridge, tuned resonant circuits (Heathman, 1993) or other capacitance measurement devices. The dielectric constant can then be calculated and regression equations calibrated to different field conditions can then be used to determine the volumetric water content from the dielectric constant. This method can be a simple and affordable method of measuring water content but errors can occur if there is appreciable electrical conductivity in the soil or if air gaps are present between the electrodes and the soil sample. An example of a capacitance probe is the Surface Capacitance Insertion Probe (SCIP) of the Institute of Hydrology (Cuenca et al., 1996).

2.2.4.5 Magnetic Field Techniques: Induced Fields (Inductive)

There are two methods that use the principle of magnetic induction to sense for water in the soil or subsurface media: the continuous method, and the pulsed method.

The first method involves a continuous AC current flowing in a loop on the soil surface. This loop creates magnetic fields, which penetrate the soil, and in turn induce currents in the soil at magnitudes that are proportional to the amount of electrical conductivity in the soil. These induced currents create magnetic fields of their own which oppose the driving field. These opposing fields can be detected on a second loop antenna on the soil surface and conclusions then drawn as to the amount of water in the soil. This continuous method is useful at shallow depths of less than 10 meters.

The pulsed method involves pulsing a current on and off on a single loop at the soil surface and then waiting for an induced response from a lower resistance loop path somewhere in the soil depths. The length of time it takes the induced response to return to the surface gives information on how deep the water is. The same loop antenna at the soil surface can be used to detect the returning pulse. This method can be used for depths of 30 meters up to 1 kilometer.

A disadvantage of these induced field methods is that they assume that any conductive loops in the soil are due only to water which is not necessarily true. If there are metals in the soil such as Iron then current loops can be induced in those regions, fooling the measurement system and user into thinking that water has been located. Also if there are magnetic materials in the soil they can also distort the path of the magnetic field lines of flux causing measurement errors.

Through field evaluation Sheets and Hendrickx (1995) concluded that electromagnetic induction is a viable method for non-invasive soil water content

measurements as long as the soil temperature is accounted for. They concluded that the method was quite accurate when compared to neutron probe readings. Electromagnetic induction methods still need to be calibrated initially at each site with some other method such as gravimetric or neutron thermalization.

2.2.4.6 Magnetic Field Techniques: Fluctuations in Earth's Magnetic Field

Another magnetic method which may be useful in locating water is the observation of anomalies in the Earth's magnetic field. There are maps which indicate what the approximate strength of the Earth's magnetic field should be at as well as its alignment direction for any given location on Earth. The field changes with time and so recent maps need to be used. Also the field varies on a repetitive 24 hour cycle. The flux density of the Earth's magnetic field is typically around 50000 nanoTesla although localized variations can occur due to magnetic materials. An instrument called a proton precession magnetometer can be used to detect flux density changes of as little as 0.1 nanoTesla and therefore can be used to detect changes caused by either local magnetic materials or local non-magnetic materials relative to the surroundings. Localized changes or perturbations in the Earth's magnetic field over a particular area would indicate changes in the magnetic content of the soil below.

Water, however, is typically slightly diamagnetic or basically non-magnetic (unless magnetic materials are in solution) and therefore would have little effect on the external magnetic field. The only possible way in which this method might be used to detect water would be if the dominant solids in the soil were magnetic (i.e. iron) and there was a non-magnetic water aquifer at one location that showed up as a slight localized reduction in magnetic flux density. The method could not be used to measure actual water content, however, as there is no way to distinguish water from air since both have relative magnetic permeabilities near 1. This method would have additional inaccuracies if there was

heterogeneity in the soil magnetic materials (i.e. non-homogeneous mixture of magnetic and non-magnetic materials) or if power lines are nearby. Therefore this method is not suitable for measuring water content.

2.2.4.7 *Electromagnetic Wave Propagation & Reflection Techniques: Time Domain Reflectometry (TDR)*

Time Domain Reflectometry can be used to determine the soil water content indirectly by making use of the principle that water molecules are strongly polar and therefore increasing water content in the soil results in an increase in the soil dielectric constant. An electromagnetic step waveform, with frequency components in the RF and Microwave bands, is propagated down a transmission line with the soil serving as the dielectric medium in the line. The line is open circuited at the end and so the propagating wave is reflected and returns to the source. The dielectric constant of the medium is a function of the time of travel of the waveform down and back the transmission line. A regression or calibration equation is then used to determine water content from the dielectric constant. TDR is discussed in greater detail in the discussion section as well as with the proposed model.

TDR offers several advantages: TDR systems respond rapidly to changing soil moisture and have very fast measurement times. TDR measurements can be automated very easily and are very accurate if salinity is absent or low. TDR systems can also be used to measure electrical conductivity and therefore estimate salinity. There is present research being conducted on non-invasive TDR probes (Selker et al., 1993; Flugstad, 1995). TDR offers great promise in balancing the design goals of reduced soil disturbance, measurement accuracy and resolution, measurement automation, speed of measurement, imaging area, and cost of measurement and is the basis for the ongoing research project proposed in this report.

The disadvantages of TDR in its present form include accuracy problems in the presence of high electrical conductivity as well as soil disturbance due to the requirement of access tubes or penetrating probes. This method also requires expensive instrumentation at this time although recent research (Flugstad and Selker, 1996) shows that there is potential for reducing the cost of that instrumentation by using only frequency ranges that are meaningful to TDR water content measurement results.

2.2.4.8   *Electromagnetic Wave Propagation & Reflection Techniques: Ground Penetrating Radar (GPR)*

This method can be used to locate water by sending an RF electromagnetic wave into a soil and looking for the return of reflected signals. The wave will reflect at an impedance boundary (see discussion) and return at a trajectory angle equal and opposite to the angle of incidence. The speed of the traveling wave is proportional to the inverse square root of the dielectric constant in the soil. Carefully spaced receivers along the surface of the earth can detect the reflected wave and triangulation methods used to determine at what depth the impedance boundary occurs. Also, by knowing the angle of travel of the wave and the depth of the reflection point along with the length of time it takes the pulse to return to the surface of the soil, the velocity of the traveling wave can be determined. This velocity theoretically gives information on the dielectric constant of the medium above the reflecting boundary (if electrical conductivity is low) and therefore potentially allows for the determination of water content. One equation to quantify the amount of reflected signal is given as follows for a normal incident wave (Selker, 1993):

$$\text{Reflection Coefficient} = \left(\frac{n_1 - n_2}{n_1 + n_2} \right)^2 \tag{15}$$

where n_1 and n_2 are the indices of refraction for the media on each side of the impedance boundary. The index of refraction for a boundary is the ratio of the phase velocity of

electromagnetic waves in free space to the phase velocity of the wave in the particular media. As will be seen in the discussion on electromagnetic theory section, the equations for reflection get much more complex when electric conductivity and complex permittivity are present. The amount of electrical conductivity will determine how deep a particular frequency can penetrate into the soil. Also the wavelength of the signal will determine the amount of resolution of the measurement (on the order of 1/4 wavelength). The higher the frequency the shallower the depth of penetration but the greater the measurement resolution. Angular trajectories, with transmitter and receiver at different locations can give information about the depth of an aquifer by triangulation. Ground Penetrating Radar is an good method for locating groundwater aquifers or even metals non-invasively and potentially could be used to determine actual water content if enough signal processing horsepower is available. More research is therefore warranted for this method.

2.2.4.9 Electromagnetic Wave Propagation & Reflection Techniques: Microwave Remote Sensing (large scale)

The methods discussed so far give information on soil moisture over relatively small areas and volumes in the field. If larger area measurements are needed, for instance to cover an entire field, then microwave remote sensing is a good choice. There are two types of remote sensing: Passive sensing and active sensing. In passive microwave remote sensing natural radiation is detected from the earth and correlated to various parameters such as cloud features, sea temperature, snow cover, surface moisture, etc. In active microwave remote sensing the electromagnetic waves are transmitted from an satellite, airplane or balloon and sent towards the earth's surface and a portion of the energy is reflected at the soil surface or slightly below it due to an impedance discontinuity. The rest of the wave energy penetrates the soil and eventually reflects at a typical major impedance boundary deeper in the ground (such as the water table) or at lesser boundaries along the way. The amount of signal energy reflected at the first reflection gives information about the dielectric constant and therefore moisture content in the upper soil horizon.

Assumptions must be made about the variation of dielectric constant with depth and what the representative depth is that contributes to the first reflection. Sometimes infrared frequencies are used in remote sensing to look for heat or vigor in plants or other thermal activity. The radar band designations used for microwave remote sensing are shown in table 1 (Avery et al., 1992; Jay et al., 1984):

Table 1
Radar band designations for microwave remote sensing

Band Designation	Frequency Range (GHz)	Wavelength Range (cm)
L	1.0 - 2.0	15.00 - 30.00
S	2.0 - 4.0	7.50 - 15.00
C	4.0 - 8.0	3.75 - 7.50
X	8.0 - 12.0	2.50 - 3.75
K_u	12.0 - 18.0	1.67 - 2.50
K	18.0 - 27.0	1.11 - 1.67
K_a	27.0 - 40.0	0.75 - 1.11

The bands most popular for use by remote sensing are the L, C, X, and K_a bands.

The advantages of this method are that a large surface area can be imaged non-invasively and that other information besides water content can be obtained depending on what frequency is chosen (i.e. temperature of objects and vigor of plants). Information can be obtained during day or night and in remote geographical locations.

Disadvantages include difficulty of interpreting the data due to numerous variables that can effect the reflected energy amount and wave trajectory. Assumptions about the impedances in the soil are often made in the development of the calibration equations for water content. The effect of complex permittivity of water in the C, X and K_a bands may affect accuracy and it is unclear whether or not it is being properly accounted for in present measurement techniques. The imaginary or loss component of the complex permittivity of water peaks at 17.8 GHz (near the top of the K_u band) but is still appreciable in the C, X, and K_a bands and should be accounted for. DC conductivity effects have little effect on the phase velocity and intrinsic impedance at those frequencies

but do have a huge effect on the depth of penetration and energy levels of the signals that have penetrated the soil and can therefore have an effect on reflected signal amplitudes from deeper in the soil. If only first reflection data is used (soil surface reflection) and reflection energy from deeper in the ground is ignored or processed out, then the effects of dc conductivity are negligible due to the frequency range but complex permittivity must still be accounted for. Weather, such as cloud cover, snow cover, as well as variations in the ground cover or plant size and type can also have an effect on measurement accuracy and must be properly accounted for. Lower frequencies (i.e. L-band) perform better than higher frequencies in the presence of clouds and/or snow cover. Extreme weather can prevent data collection altogether. This method is also expensive to use and depends on flight schedules of airplanes or satellite orbit schedules which limit when measurements can be made. Some other method such as TDR or Neutron Probes must be used on the ground to provide calibration data to enable proper interpretation of the remote sensing information.

2.2.4.10 Electromagnetic Wave Propagation & Reflection Techniques: Microwave Backscattering (small scale)

On a smaller scale microwave radiation can be propagated into a medium to obtain information on the water content of soil samples, food or other items non-invasively by measuring either transmission or reflection properties of these waves about the medium. Comparing the amount of signal that is transmitted into the medium to the amount of signal that is reflected at the surface can give information about the dielectric constant or water content of the medium. Again, great care must be taken in the presence of complex permittivity (see discussion section) in interpreting the results of the measurement. An example of a commercially available product is the Model 1800 by Spatial Dynamics Applications which operates at 1.8 GHz or in the L band of the microwave range.

2.2.4.11 Quantum Mechanic Techniques:
Nuclear Magnetic Resonance (NMR)

NMR makes use of the measurable effects of changing quantum mechanic energy states in the nucleus of atoms. Atoms with odd numbers of protons or neutrons (such as hydrogen) possess what is termed "spin". These spins have finite numbers of directions and magnitudes (quantum states). If a medium is placed in a strong constant magnetic field (typically 0.1 Tesla up to 6 Tesla) then all these nuclear spins will align themselves with the external magnetic field. If in addition to the magnetic field an external RF frequency source (1 MHz to 100 MHz range) sends a wave into the medium at a frequency equal to the nuclear magnetic resonance frequency for hydrogen at the given magnetic field strength, then the spins will be shifted out of alignment to either an orthogonal or antiparallel alignment (i.e. higher quantum states). If the RF source is then turned off, the nuclear spins of the hydrogen atoms will relax or drop down to the lower quantum states and realign with the constant external magnetic field. This relaxation will lead to the release of RF electromagnetic waves at the nuclear magnetic resonance frequency. The amount of energy as well as the source of these waves can be detected and determination made about the amount and location of hydrogen in the medium. This can give information as to how much water is in a medium. This is explored in greater depth in the discussion section.

An advantage of NMR is the potential for a high resolution non-invasive method of measuring water content. Another advantage is the potential to measure water potential in addition to water content (Tollner et al., 1987).

The major disadvantages of this method are: (1.) the difficulty in maintaining a uniform dc magnetic field in a heterogeneous soil; (2.) the depth of penetration limitations of the RF frequency (especially where conductivity is appreciable); (3.) the amount of information that must be post processed to extract water content; and (4) the high cost of the equipment required.

3. DISCUSSION: ELECTROMAGNETIC THEORETICAL BACKGROUND

In this chapter the theories of electromagnetics, and quantum mechanics as well as scattering (S) parameter network theory are discussed in greater depth along with their application towards soil moisture measurement techniques. The proposed ongoing research will be investigating the use of a TDR model based on large portions of two of these theories: electromagnetic wave propagation theory as well as S-parameter network theory. Quantum mechanics is also discussed due to the potential of developing a non-invasive soil water content and water potential measurement technique that combines quantum mechanics with electromagnetics (NMR). NMR soil moisture measurement techniques are therefore deserving of more study, but that will be left to other researchers.

3.1 Foundation: Maxwell's Equations

Maxwell's equations (shown below in both integral & differential form) relate time and space varying electric and magnetic fields to each other utilizing the parameters of electric permittivity ε, magnetic permeability μ, and electrical conductivity σ. Maxwell's equations in integral form are given as follows:

$$\oint_C \mathbf{E} \bullet d\mathbf{l} = -\frac{\partial}{\partial t} \iint_S \mathbf{B} \bullet d\mathbf{S} \tag{16}$$

$$\oint_C \mathbf{H} \bullet d\mathbf{l} = \iint_S \mathbf{J} \bullet d\mathbf{S} + \frac{\partial}{\partial t} \iint_S \mathbf{D} \bullet d\mathbf{S} \tag{17}$$

$$\oiint_S \mathbf{D} \bullet d\mathbf{S} = \iiint_V \rho \, dV \tag{18}$$

$$\oiint_S \mathbf{B} \bullet d\mathbf{S} = 0 \tag{19}$$

where   H = magnetic field intensity (amperes/meter)

B = magnetic flux density (webers/square meter)

E = electric field intensity (volts/meter)

D = displacement flux density (coulombs/square meter)

J = current density (amperes/square meter)

ρ = charge density (coulombs / cubic meter)

L = length (meters)

s = surface area (square meters)

v = volume (cubic meters)

and   D = ϵ E   where ϵ = electrical permittivity (farads/meter)

B = μH   where μ = magnetic permeability (henries/meter)

J = σ E   where σ = electrical conductivity (mho's/meter)

Alternatively Maxwell's equations can also be written in differential form as follows:

$$\nabla \times E = -\frac{\partial B}{\partial t} \tag{20}$$

$$\nabla \times H = J + \frac{\partial D}{\partial t} \tag{21}$$

$$\nabla \cdot D = \rho \tag{22}$$

$$\nabla \cdot B = 0 \tag{23}$$

3.2 Electric Field Parameters

Electric permittivity ε is a measure of a material's ability to create electric dipoles (due to polarized molecules) in the presence of an external electric field. These dipoles align themselves with the external field and in turn create electric fields of their own that oppose the external electric field. The stronger these dipoles (and the more of them) the more the external field is attenuated within the material, and the greater the "dielectric". The amount of dielectric behavior of a medium can be quantified by the relative electric permittivity or dielectric constant ε_r given as follows:

$$\varepsilon_r = \frac{\varepsilon}{\varepsilon_0} \tag{24}$$

where ε_0 is the permittivity of free space and is equal to 8.854E-12 Farads/Meter.

If two conducting plates are placed on opposite sides of the outside of a dielectric, electric charge is stored when a voltage is applied to the plates. If the electric permittivity is high more charge is stored for a given voltage due to the greater attenuation of the electric field within the dielectric due to the opposing dipoles. The net electric field is the voltage divided by the thickness of the dielectric. The quantity of charge that can be stored for a given voltage is referred to as the capacitance of the dielectric medium. The capacitance (Coulombs/Volt or Farads) is proportional to the geometrical properties of the electrodes and the medium between them as well as proportional to the electric permittivity of the medium by an equation of the following form:

$$C = \varepsilon K' \tag{25}$$

Where K' is a function of the geometrical properties of the capacitor and is directly proportional to the surface area of applied charge (or conducting plate area) and is inversely proportional to the thickness of the dielectric material. This can be compared to

equations 13 and 14 for the capacitance probe to measure water content. By measuring the capacitance of a select volume of soil one can determine its dielectric constant. It has been shown that soil water content is proportional to this dielectric constant by an empirically derived equation of the following form (Topp et al., 1980):

$$\theta = A_0 + A_1\varepsilon_r + A_2\varepsilon_r^2 + A_3\varepsilon_r^3 \tag{26}$$

where A_0 thru A_3 are empirically derived constants (linear regression) and ε_r is the dielectric constant. It is shown later that the phase velocity of an electromagnetic wave can be traced back to the dielectric constant under a certain set of assumptions which is the basis behind TDR soil moisture content measurements (see section on electromagnetic wave effects).

The electric permittivity ε can be complex, as shown in equation 27, due to high frequency loss mechanisms not accounted for in DC conductivity such as the ability of a medium to absorb energy due to the self resonance of polar molecules such as water at microwave frequencies.

$$\varepsilon = \varepsilon' - j\varepsilon'' = \varepsilon_r'\varepsilon_0 - j\varepsilon_r''\varepsilon_0 = \varepsilon_r^*\varepsilon_0 \tag{27}$$

where
ε' = real or energy storage term of electric permittivity

ε'' = imaginary or loss term of electric permittivity

ε_r' = real or energy storage term of dielectric constant

ε_r'' = imaginary or loss term of dielectric constant

ε_r^* = overall complex dielectric constant

j = $\sqrt{-1}$

A widely used mathematical model for the complex electric permittivity is the Cole-Cole model (neglecting dc conductivity and assuming no spread in the relaxation frequencies) and is shown as follows (Heimovaara, 1994):

$$\varepsilon' = \varepsilon_0 \left[\varepsilon_\infty + \frac{\varepsilon_s - \varepsilon_\infty}{1 + \omega^2 \tau^2} \right] \tag{28}$$

$$\varepsilon'' = \frac{\omega \varepsilon_0 \tau (\varepsilon_s - \varepsilon_\infty)}{1 + \omega^2 \tau^2} \tag{29}$$

where ε_s = Low frequency dielectric constant

ε_∞ = High frequency dielectric constant

τ = Relaxation time of the polar water molecule H_2O.

Using equations 27 - 29, plots of the real and imaginary components of the complex dielectric constant (ε_r' and ε_r'' respectively) vs. frequency are shown in figure 1:
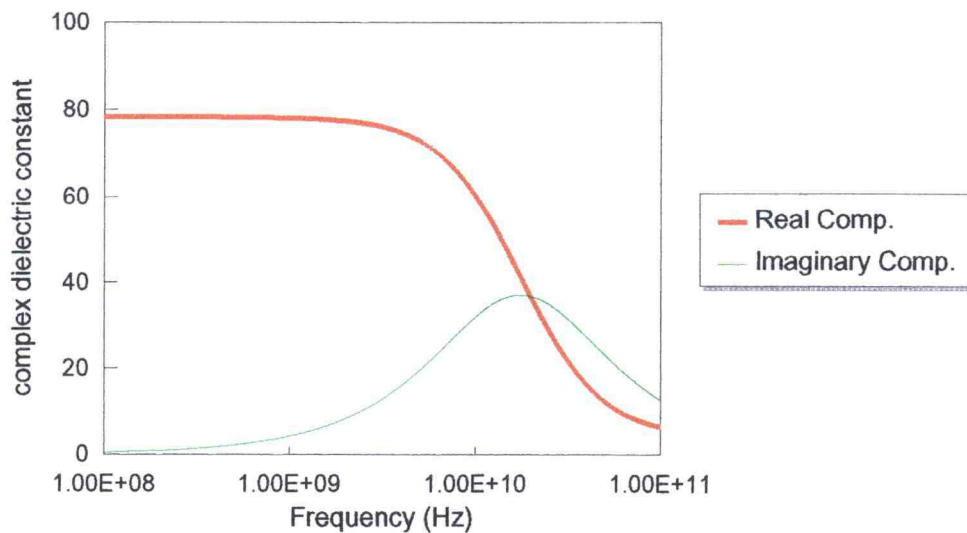

Figure 1.   Real and imaginary components of the complex dielectric constant of water vs. frequency.

In the case of a mixture of solids, water, and air in the soil, other factors may be needed to accurately model this imaginary component of the overall dielectric constant, especially at low water contents, due to the complex mixing of these three components.

Electrical Conductivity σ is a measure of the ability of an externally applied electric field to produce a current in a medium opposite to the direction of the field. It is governed by the following equation:

$$\sigma = \frac{J_c}{E} \tag{30}$$

where J_c is the current density (A/m^2), σ is the electrical conductivity (S/m), and E is the electric field intensity (V/m). Electrical conductivity is important in soil moisture measurements in that water often contains ions (especially in saline conditions) that increase its conductivity and in turn attenuate propagating electromagnetic waves. Soils with metals or other conductive elements or compounds will attenuate propagating electromagnetic waves as well. So if a soil is very conductive there will be a severe limitation as to what depth in the soil electromagnetic waves can be used to measure soil properties. Lower frequencies can penetrate deeper than higher frequencies and this is called the skin effect. Bulk conductivity or resistivity (inverse of σ) of the soil can be measured under certain conditions to determine the location and depths of aquifers (relatively near the surface) by assuming that the water is conductive and the soil solids are not.

3.3 Magnetic Field Parameters

Magnetic permeability μ is a measure of a material's ability to create magnetic dipoles in the presence of an external magnetic field that either oppose (diamagnetism) or sometimes enhance (paramagnetism) the applied external field. Sometimes a material may

be magnetized even in the absence of an external magnetic field (ferromagnetism). These micro-magnets or magnetic dipoles are the result of electron orbit paths becoming coherent in orientation (or aligning themselves) relative to those of other molecules as opposed to being random resulting in a net magnetic field. This magnetic field component is then added (subtracted if diamagnetic) to the external magnetic field flux density to give a new magnetic flux density. For a given current around a loop surrounding a material the same magnetic field intensity H is obtained, but different values of magnetic flux densities B result depending on the magnetic permeability μ. Ferromagnetic properties are found in Iron (Fe) and Nickel (Ni) and Cobalt (Co) as well as several alloys of these elements and other elements. The measure of the amount of magnetic flux density that can be induced by this external current loop is called the inductance of the loop. The inductance is also proportional to geometrical factors as well as the number of turns of wire around the material and is proportional to the ratio of B/H. The magnetic permeability can be separated into two parts (in an analogous fashion to the electric permittivity) as given by equation 31:

$$\mu = \mu_r \mu_o \qquad\qquad\qquad (31)$$

where $\quad \mu_r$ = relative permeability

$\qquad\qquad\qquad = 1 + \chi_m$

where $\quad \chi_m$ = the magnetic susceptibility of the material

$\qquad\qquad \chi_m$ = -10E-8 to -10E-4 for diamagnetic materials (negative)

$\qquad\qquad \chi_m$ = +10E-7 to +10E-3 for paramagnetic materials (positive)

$\qquad\qquad \chi_m$ = +100 to +10000 or more for ferromagnetic materials (positive)

μ_o = magnetic permeability of free space = 4π x 10E-7 = 1.26E-6 Henries/meter.

$H = B/(\mu_r\mu_o)$.   H = Magnetic Field Intensity (amperes/meter)

B = Magnetic Flux Density (webers/square meter) or Tesla or 10E4 Gauss.

L = G'N(B/H) = Inductance in Henries.   N = number of turns of wire

$\qquad\qquad\qquad\qquad\qquad\qquad\qquad$ G' = geometrical factors

In terms of application to soil moisture measurements it will be shown that magnetic materials in the soil greatly effect the propagation characteristics of electromagnetic waves and can therefore distort information gained by other electromagnetic methods. Pure (distilled) water is slightly diamagnetic and therefore has a relative permeability very close to (just under) one and so its magnetic properties by itself can't be used to distinguish wet soil from dry soil or moisture content. If water contains ferromagnetic materials in solution or as suspended solids then it might exhibit some magnetic properties but it is still likely that the relative permeability in that water would be close to one. The use of inductance or inducing current loops in the soil and then detecting the resulting opposing fields can be used to locate water if it is assumed that the water contains ions and is more conductive than its surroundings. This induction method is probably the best way to use magnetic field methods to locate water.

3.4 Electromagnetic Wave Propagation Models

In this section, an overview of the theoretical models for uniform plane wave propagation is given, as well as the special case of wave propagation down a parallel conductor transmission line.

3.4.1 Uniform Plane Waves

Consider a homogeneous volume of soil with a given value of electrical conductivity σ, electric permittivity ε, and magnetic permeability μ. Assume the simplified case of an infinite alternating current plane in the xy plane bisecting this medium, giving rise to electromagnetic waves radiating away and propagating in the positive and negative z-directions from the xy plane. These waves are called uniform plane waves. In this case, a manipulation of Maxwell's equations (16-23) results in the following two partial differential equations called the wave equations (Rao, 1977; Eyges, 1972; Jin, 1993.):

$$\nabla^2 \mathbf{E} = \mu \frac{\partial}{\partial t}[\sigma \mathbf{E} + \varepsilon \frac{\partial \mathbf{E}}{\partial t}] \quad \text{or} \quad \nabla^2 \mathbf{E} = j\omega\mu(\sigma + j\omega\varepsilon)\mathbf{E} = \gamma^2 \mathbf{E} \quad (32)$$

$$\nabla^2 \mathbf{H} = \mu \frac{\partial}{\partial t}[\sigma \mathbf{H} + \varepsilon \frac{\partial \mathbf{H}}{\partial t}] \quad \text{or} \quad \nabla^2 \mathbf{H} = j\omega\mu(\sigma + j\omega\varepsilon)\mathbf{H} = \gamma^2 \mathbf{H} \quad (33)$$

where the overall propagation constant is defined by equation 34:

$$\gamma = \sqrt{j\omega\mu(\sigma + j\omega\varepsilon)} = \sqrt{j\omega\mu(\sigma + \omega\varepsilon'' + j\omega\varepsilon')} \equiv \alpha + j\beta \quad (34)$$

and where ω is the angular frequency (radians/sec), α is the attenuation constant (Nepers/meter), and β is the phase constant (radians/meter). The parameters α and β are given as follows:

$$\alpha = \omega\sqrt{\frac{\mu\varepsilon'}{2}\left(\sqrt{1 + \left(\frac{\sigma + \omega\varepsilon''}{\omega\varepsilon'}\right)^2} - 1\right)} \quad (35)$$

$$\beta = \omega\sqrt{\frac{\mu\varepsilon'}{2}\left(\sqrt{1 + \left(\frac{\sigma + \omega\varepsilon''}{\omega\varepsilon'}\right)^2} + 1\right)} \quad (36)$$

The general solutions to equations 32 and 33, for waves propagating in the positive and negative z-direction away from this infinite current plane are both sine waves in time and space, but with amplitudes orthogonal in space which are both orthogonal to the propagation direction of the sine wave. These solutions are given as follows (Rao, 1977):

$$\mathbf{E}_x(z, t) = [Ae^{-\alpha z}\cos(\omega t - \beta z + \theta) + Be^{\alpha z}\cos(\omega t + \beta z + \phi)] \quad (37)$$

$$\mathbf{H}_y(z, t) = [\frac{A}{|\eta|}e^{-\alpha z}\cos(\omega t - \beta z + \theta - \xi) - \frac{B}{|\eta|}e^{\alpha z}\cos(\omega t + \beta z + \phi - \xi)] \quad (38)$$

θ, ϕ, and ξ are additional phase shift terms of the positive and negative traveling waves and between the magnetic and electric field terms and are assumed equal to zero in this thesis. η is the intrinsic impedance and is given by:

$$\eta = \sqrt{\frac{j\omega\mu}{\sigma + \omega\varepsilon'' + j\omega\varepsilon'}} \tag{39}$$

Equations 37 and 38 are time domain solutions. In the frequency domain the solutions are shown by equations 40 and 41 (positive z terms only and neglecting additional phase shifts) which are readily obtained from equations 32 and 33:

$$E(z,\omega) = Ae^{-\gamma z} \tag{40}$$

$$H(z,\omega) = \frac{A}{\eta} e^{-\gamma z} \tag{41}$$

A common ratio that shows up in these equations is the ratio of the electric field energy loss (or conductive) terms to the electric field energy storage (or dielectric) term. This ratio is called the loss tangent, L_T, and is defined as follows:

$$L_T = \frac{\sigma + \omega\varepsilon''}{\omega\varepsilon'} \tag{42}$$

Notice that for an insulator ($L_T \ll 1$), that $\alpha = 0$, $\beta = \omega\sqrt{\mu\varepsilon'}$, and $\eta = \sqrt{\frac{\mu}{\varepsilon'}}$.

Equations 37 and 38 show propagating waves in both the positive and negative z-directions with electric and magnetic field components oriented in the x and y directions respectively. The waves attenuate over distance z in an exponential manner with the decay constant equal to α. The waves propagate at a velocity v_p (phase velocity) given by equation 43:

$$v_p = \frac{\omega}{\beta} = \cfrac{1}{\sqrt{\cfrac{\mu \varepsilon '}{2} \left(\sqrt{1 + \left(\cfrac{\sigma + \omega \varepsilon ''}{\omega \varepsilon '} \right)^2} + 1 \right)}}$$ (43)

Notice that $v_p = \dfrac{1}{\sqrt{\mu \varepsilon '}}$ if $L_T \ll 1$.

3.4.2 Transmission Line Model

Consider a parallel conductor transmission line with a given series inductance L per unit length, shunt capacitance C per unit length, series resistance R per unit length, and shunt conductance G per unit length. The distributed model for this type of transmission line is shown in figure 2, where dz is the differential length of the transmission line section.
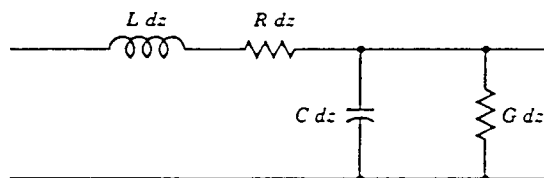

Figure 2. Distributed model for a transmission line showing one differential section.

From Maxwell's equations, the overall propagation constant γ for electromagnetic waves propagating down a transmission line is (Rao, 1977; Ramo et al., 1994):

$$\gamma = \sqrt{(R + j\omega L)(G + j\omega C)} \tag{44}$$

For a parallel wire transmission line the with a spacing s and a wire diameter d the following values for R, G, L and C can be derived (Ramo et al., 1994):

$$C = \frac{\pi \varepsilon'}{\text{Cosh}^{-1}\left(\frac{s}{d}\right)} \tag{45}$$

$$L = \left(\frac{\mu}{\pi}\right)\text{Cosh}^{-1}\left(\frac{s}{d}\right) \tag{46}$$

$$G = \frac{\pi(\sigma + \omega\varepsilon'')}{\text{Cosh}^{-1}\left(\frac{s}{d}\right)} \tag{47}$$

$$R = \left(\frac{2R_s}{\pi d}\right)\left[\frac{\frac{s}{d}}{\sqrt{(s/d)^2 - 1}}\right] \tag{48}$$

Where Rs = the skin effect surface resistivity of the metal wire and is given as follows:

$$R_s = \sqrt{\frac{\omega \mu_c}{2\sigma_c}} \tag{49}$$

Putting equations 45 - 48 into equation 44, assuming s >> d, the following expression for total propagation constant γ is obtained:

$$\gamma = \sqrt{\left(\frac{2\,R_s}{\pi\,d} + \frac{j\omega\,\mu\,\text{Cosh}^{-1}\left(\frac{s}{d}\right)}{\pi}\right)\left(\frac{\pi\,(\sigma + \omega\varepsilon\,")}{\text{Cosh}^{-1}\left(\frac{s}{d}\right)} + \frac{j\omega\,\pi\,\varepsilon\,'}{\text{Cosh}^{-1}\left(\frac{s}{d}\right)}\right)} \qquad (50)$$

For gold-plated or other high quality conductors the skin effect surface resistivity R_s can typically be neglected below 100 GHz (TDR systems operate at less than 20 GHz) from which it follows that equation 50 reduces to the same expression as that for the overall propagation constant for uniform plane waves given in equation 34. Therefore, for wave propagation down a parallel wire transmission line, the expressions for the attenuation constant α and phase constant β, and phase velocity v_p are equivalent to those for the uniform plane wave case.

3.4.3 Dispersion Effects

In conditions of high salinity or high electrical conductivity, at frequencies where the loss tangent >> 1, the expression for phase velocity (equation 43) reduces to:

$$v_p = \sqrt{\frac{2\,\omega}{\mu\,(\sigma + \omega\varepsilon\,")}} \qquad \text{when } L_T \gg 1 \qquad (51)$$

which reduces to equation 52 at lower frequencies where σ >> ωε " :

$$v_p = \sqrt{\frac{2\,\omega}{\mu\,\sigma}} \qquad \text{when } L_T \gg 1 \ \& \ \sigma \gg \omega\varepsilon\," \qquad (52)$$

Equation 52 shows that for a good conductor the phase velocity is dependent on frequency of the signal and conductivity of the medium instead of the dielectric constant. This implies that the standard procedure of measuring phase velocity is not sufficient to determine water content when $L_T \gg 1$. Examination of equation 43 shows that as frequency goes up, (for a given ele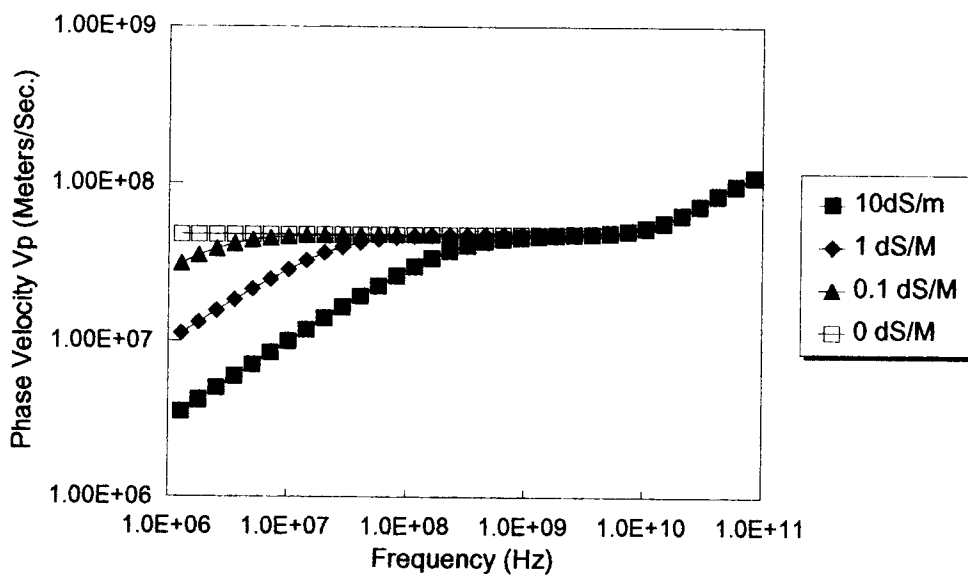ctrical conductivity), phase velocity will increase until it reaches a maximum value which is then independent of conductivity and frequency (in the absence of complex permittivity) and is equal to $\frac{1}{\sqrt{\mu \varepsilon}}$, (i.e. an insulator or non-conductive soil with the same water content). Therefore the effect of equation 52 is the retarding or slowing of the low frequency components in a traveling pulse, relative to the high frequency components, which can lead to dispersion in time and space of the Fourier components of the pulse. The behavior of phase velocity vs. frequency and conductivity for the case of a dry soil ($\varepsilon_r = 4$) and a very wet soil ($\varepsilon_r = 40$) is shown in figure 3. Low frequency variations in phase velocity are caused by dc electrical conductivity and high frequency variations in phase velocity are caused by variances in the complex permittivity.
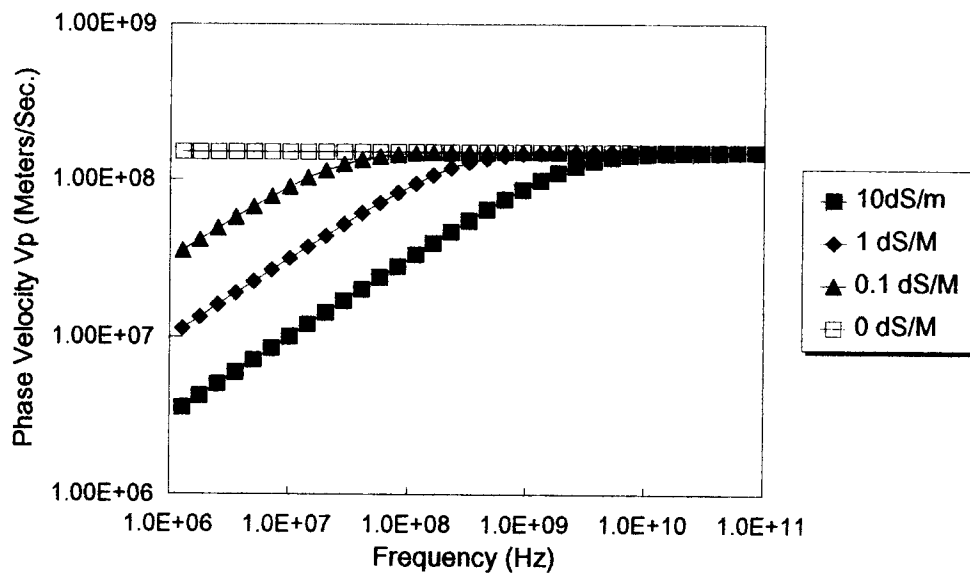
Figure 3. Phase velocity vs. frequency and electrical conductivity for a.) dry soil
($\varepsilon_r = 4$) and b.) very wet soil ($\varepsilon_r = 40$) conditions.

3.4.4 Attenuation Effects

Equation 35 shows that increased conductivity, as well as increased complex permittivity, increase wave attenuation of higher frequency components. Thus higher frequencies do not penetrate as far into conductive soils, or other conductive media, as can lower frequencies. (This is why submarines use extremely low frequencies in their communications.) The depth of penetration by a particular frequency is characterized by the skin depth δ:

$$\delta = \frac{1}{\alpha} = \frac{1}{\omega \sqrt{\dfrac{\mu \varepsilon'}{2} \left(\sqrt{1 + \left(\dfrac{\sigma + \omega \varepsilon''}{\omega \varepsilon'} \right)^2} - 1 \right)}} \qquad (53)$$

Notice that $\qquad \delta = \dfrac{\sqrt{2}}{\sqrt{\omega \mu (\sigma + \omega \varepsilon'')}} \qquad$ if $L_T \gg 1$.

The skin depth corresponds to the depth of penetration at which the wave has been attenuated to 37% (1/e) of its initial amplitude. For a good conductor ($L_T \gg 1$), and at lower frequencies where $\sigma \gg \omega \varepsilon''$, δ is inversely proportional to the square root of frequency. The skin depth goes to ∞ if both the conductivity and imaginary component of the complex permittivity go to zero (insulator or poor conductor where $L_T \ll 1$). So soils that are poor conductors can be penetrated further by electromagnetic waves than soils that are good conductors. A few times the skin depth can be used as an upper bound on the region of influence about a probe when attenuation limitations dominate over probe geometry limitations.

In the presence of non-zero electrical conductivity, and at high frequencies (in the absence of complex permittivity), L_T drops back below one and the attenuation factor α of a propagating wave in a transmission line approaches the maximum value shown in

equation 54 (derived by performing a Taylor series expansion or binomial expansion of equation 44 and taking the first order terms of the real part of the result (Magnusson et al., 1992)):

$$\alpha \cong \frac{R}{2\sqrt{L/C}} + \frac{G\sqrt{L/C}}{2} \qquad \text{when } L_T \ll 1 \text{ but } \sigma > 0 \qquad (54)$$

Again if the probe series resistivity R is neglected (i.e., assume that the shunt loss terms in the dielectric dominate over the series loss terms in the conductors), then equation 54 reduces to that shown in equation 55:

$$\alpha \cong \frac{G\sqrt{L/C}}{2} \cong \frac{\sigma}{2}\sqrt{\frac{\mu}{\varepsilon'}} \qquad (55)$$

when $L_T \ll 1$, $\sigma > 0$ & $\sigma \gg \omega\varepsilon''$.

Equation 55 is a constant, independent of frequency, and represents the maximum value of attenuation constant α that exists for a given conductivity and dielectric constant in the absence of complex permittivity.

Attenuation is therefore greatest at high frequencies as compared with dispersion which shows up more at lower frequencies when dc conductivity is high. Additional dispersion can occur at microwave frequencies due to the complex permittivity of water but this dispersion is typically masked by the high attenuation also occurring at those frequencies. The behavior of the attenuation constant α vs. frequency and dc conductivity for a wet and dry soil is shown in figure 4.
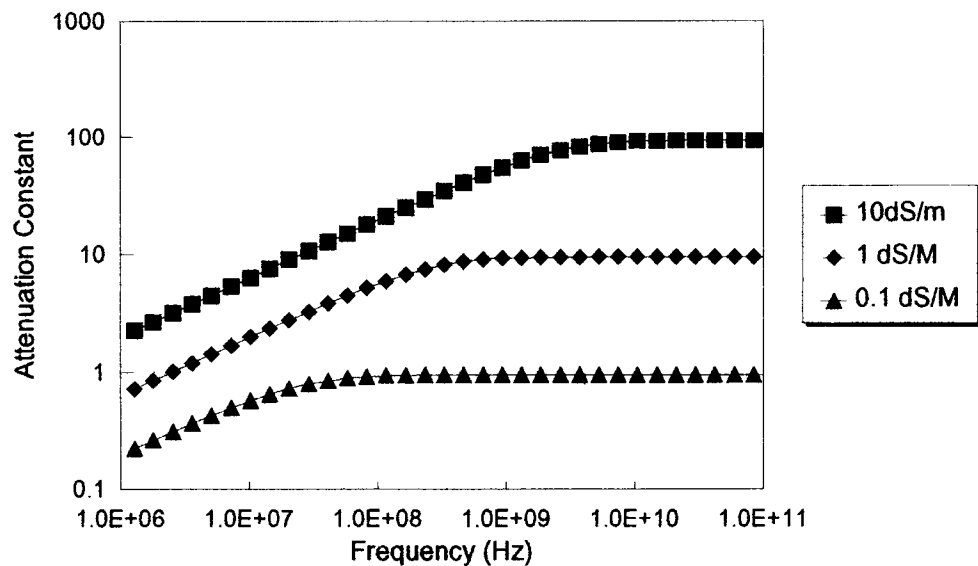
a.)
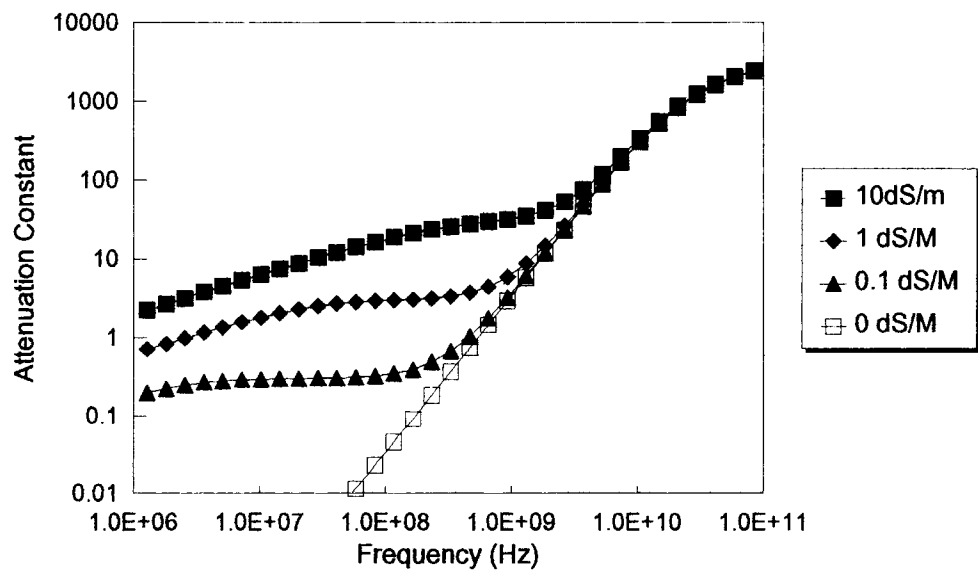
b.)

Figure 4. Attenuation constant vs. frequency and electrical conductivity for a.) dry soil
($\varepsilon_r = 4$) and b.) very wet soil ($\varepsilon_r = 40$) conditions.

3.4.5 Reflection Effects

Boundary conditions, which include changes in ε, μ and σ, can dictate that the solutions to equations 32 and 33 will exhibit terms of both reflection and transmission at the interface. This can be described by an impedance change across the boundary. The characteristic impedance of a transmission line is given by (Ramo et al., 1994):

$$Z = \sqrt{\frac{R + j\omega L}{G + j\omega C}} \qquad (56)$$

For a parallel wire transmission line, the characteristic impedance is given by equation 57, which is obtained using the expressions in equations 45 through 48 and plugging them into equation 56 and neglecting the series resistance R:

$$Z = \frac{1}{\pi} \text{Cosh}^{-1}\left(\frac{s}{d}\right)\sqrt{\frac{j\omega\mu}{\sigma + \omega\varepsilon'' + j\omega\varepsilon'}} = \frac{1}{\pi} \text{Cosh}^{-1}\left(\frac{s}{d}\right)\eta \qquad (57)$$

For the case of $L_T \gg 1$ and conductivity dominating over complex permittivity (i.e., saline soils & low frequencies) equation 57 reduces to the following:

$$Z = \frac{1}{\pi} \text{Cosh}^{-1}\left(\frac{s}{d}\right)\sqrt{\frac{j\omega\mu}{\sigma}} \quad \text{when } L_T \gg 1 \, \& \, \sigma \gg \omega\varepsilon'' \qquad (58)$$

At high frequencies (in the absence of complex permittivity) or when $L_T \ll 1$, the expression reduces to the following:

$$Z = \frac{1}{\pi} \text{Cosh}^{-1}\left(\frac{s}{d}\right)\sqrt{\frac{\mu}{\varepsilon'}} \qquad (59)$$

At high frequencies, above 10 GHz, when water contents are high, equation 57 reduces to equation 60, due to the presence of high complex permittivity:

$$Z = \frac{1}{\pi} \text{Cosh}^{-1}\left(\frac{s}{d}\right)\sqrt{\frac{j\mu}{\varepsilon''}} \tag{60}$$

Using equation 59, and assuming s >> d, an approximate expression for the characteristic impedance of a parallel wire transmission line can be obtained for low conductivity or high frequency with low complex permittivity (e.g., lower water contents & low salinities) and is given by equation 61:

$$Z = \frac{120}{\sqrt{\varepsilon_r'}} \ln\left(\frac{2s}{d}\right) \tag{61}$$

Where s is the spacing between the conductors, d is the diameter of the conductors and ε_r' is the real portion of the dielectric constant of the medium. The 120 value comes from the characteristic impedance of free space (377 ohms) divided by π; and $\text{Cosh}^{-1}(x)$ can be approximated by $\ln(2x)$ when x >> 1. Note that both equations 59 and 61 are independent of frequency. When L_T is greater than one, then equations 58 (lower frequencies) and 60 (higher frequencies) apply. When L_T is less than one, then equations 59 and 61 apply. If high conductivity is present, or where $L_T > 1$, there will no longer be a uniform characteristic impedance, but instead a frequency-dependent impedance approaching zero at low frequencies (equations 39, 57 and 58). The variance of the characteristic impedance vs. frequency and dc conductivity for wet and dry soils is shown in figure 5.
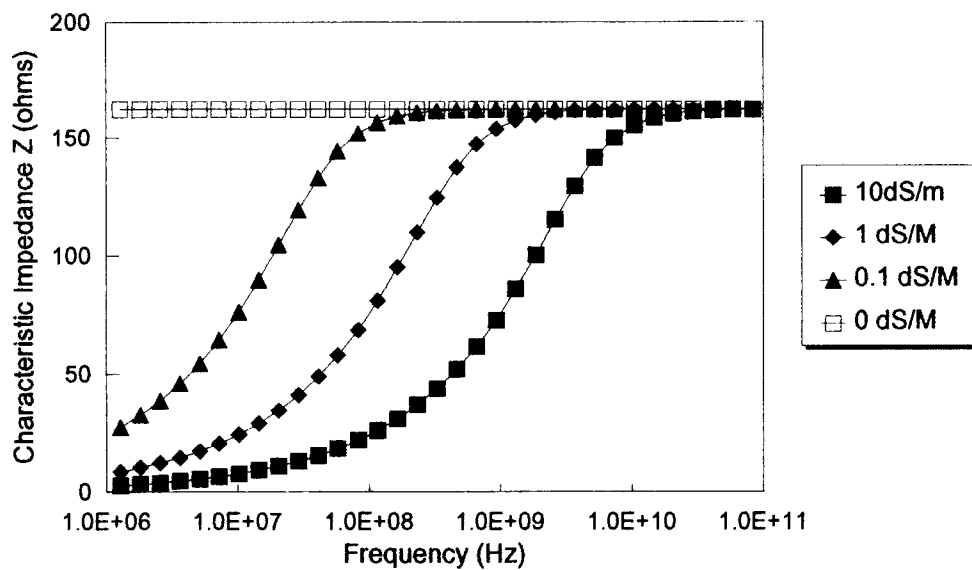
a.)
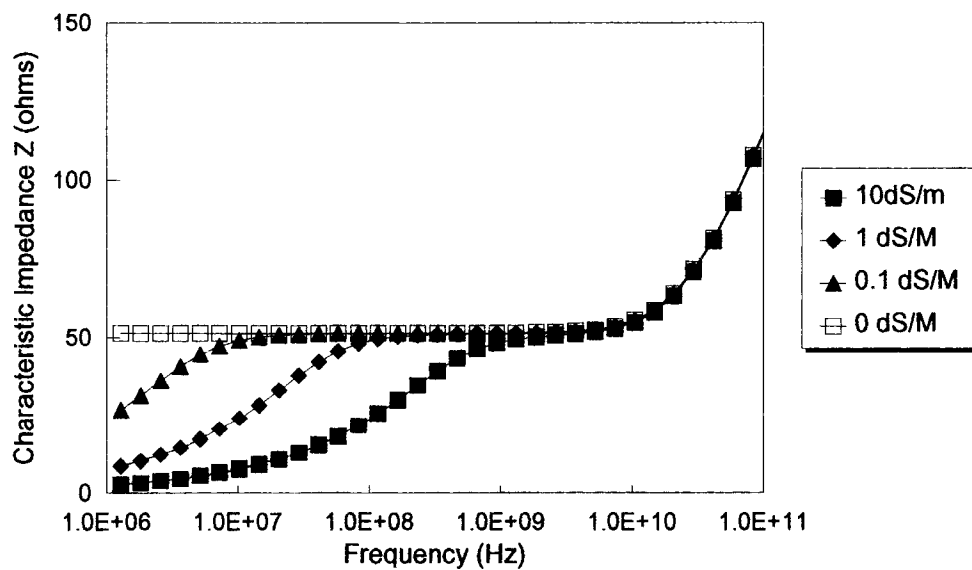
b.)

Figure 5. Characteristic impedance vs. frequency and electrical conductivity for a.) dry soil ($\varepsilon_r = 4$) and b.) very wet soil ($\varepsilon_r = 40$) conditions.

At a boundary where the impedance changes there will be reflections and they are quantified by the reflection coefficient. The reflection coefficient, Γ, is defined as the ratio of the reflected wave amplitude to the incident wave amplitude and is defined by:

$$\Gamma = \frac{Z_2 - Z_1}{Z_2 + Z_1} \tag{62}$$

Where Z_1 and Z_2 are the impedances before and after the boundary respectively.

If the angle of incidence is not orthogonal to the interface or impedance boundary, then the reflected wave will go back at an angle equal to the angle of incidence mirrored about the normal vector to the interface. Also there will be refraction or bending of the transmitted signal across the boundary.

Since soils are very heterogeneous this means that there will be a lot of reflections and bending of waves in the soil as they propagate through the medium. If the heterogeneity is at a macroscopic level and somewhat ordered (i.e. soil layers, horizons, and aquifers) and within these layers the soil is close to homogeneous then the reflection or scattering of electromagnetic waves can be used to advantage to get a profile or image of what is below. Receivers placed at regular intervals along the surface of the earth can detect reflections of waves sent into the soil and calculations can be made to determine how deep and wide the reflection inducing boundaries are beneath the surface. This is the principle behind ground penetrating radar (GPR). The resolution of the image of the soil is directly proportional to how high the penetrating frequency is of the electromagnetic wave. An electromagnetic wave can be influenced by soil dimensions down to approximately 1/4 wavelength of the wave in the soil and so that is approximately the resolution of what can be discerned. Higher frequencies give better resolutions but if there is significant electrical conductivity in the soil then the higher frequencies are attenuated more also. So a balance must be reached between these two conflicting issues. If information is desired at greater depths but resolution isn't as important (i.e. only looking

at larger horizons or aquifers) then a lower frequency might be used. If information near the surface is desired along with higher resolution then a higher frequency is the best. Spatial Dynamics, Inc. manufactures a device that sends microwaves into the soil or other objects and then senses all the reflected frequencies to make conclusions about the water content in the soil or test sample. But again, at microwave frequencies, the depth of penetration would be more severely limited, especially in the presence of high electrical conductivity. Very good spatial resolution, though, is achieved and this method performs well for small material thickness, small soil samples or shallow soil depths. Kraszewski and Nelson (1992) also showed that microwaves can be used to determine moisture content in various media.

The more complex or extensive the heterogeneity the more difficult it is to make sense of the data. This has been one of the limitations to using electromagnetic waves in soils up until recently due to the inability to post process the data and make sense of all these scattered waves (as well as attenuated waves due to conductivity). Lower cost, higher performance portable computers as well as higher performance microprocessor based data acquisition circuits are starting to remove this limitation. These developments are now being translated into a software issue. Also measurement receivers are becoming more sensitive (lower noise floors coupled with narrower bandwidths) and so smaller signals can be detected allowing for greater depths to be probed for a given soil and frequency. A possible future application is to modulate the electromagnetic wave with a low frequency pseudo-random bit stream of digital data so that the receiving waves can be signatured in time as to when they left the transmitter and how long it took to get to the receiver (i.e. detection and demodulation of the digital code). This is done to some extent with pulsed radar signals (send out a narrow pulse of an RF or microwave signal and see how long it takes to be reflected back) but could be greatly expanded upon with the present technology of electronics and computers. Another hypothesis might be that if the frequency hops around with time (i.e. digital FM modulation or just fast switching the frequency over a larger range) and a multichannel receiver is used that can discern the different frequencies then perhaps more information could be ascertained from the soil

(such as being able to separate out the soil conductivity σ from the magnetic and dielectric properties of the soil). These are all possible areas of research in the future.

3.5 Wave Propagation in Composite Media

Soils are complex media made up of several components. Generally, their constituents can be classified by the three phases of solids, liquids and gases. The solid phase is actually a mixture of several components which could include sand, silt and clay minerals as well as organic matter (both dead and alive). The liquid component could be water or oils or other fluids which could also contain ions and suspended particles in solution. The gas phase can be close to that of air or dominated by particular gases such as methane (CH_4) or carbon dioxide (CO_2). In the models developed in this thesis the solid phase is assumed to be one effective solid component with its own values of electric permittivity, magnetic permeability and electrical conductivity and therefore overall propagation constant. The organic fraction is considered low or negligible. The gas phase is assumed to be air similar to atmospheric air (77% nitrogen, 21% oxygen and 2% other components such as carbon dioxide). The liquid phase is assumed to be water with varying degrees of electrical conductivity due to ions in solution. The electric permittivity of the water component is complex and can be determined by equations 27 - 29. Therefore each constituent can have its own values of electric permittivity, magnetic permeability, and electrical conductivity and therefore overall propagation constant. Simplified mixing models for composite media using only the permittivities of the individual constituents have been developed (Roth et al., 1990) but the composite models in this thesis account for the permittivity, permeability and the conductivity of the individual constituents.

If it is assumed that all three phases of the soil act is they are in series or in a cascade fashion in an electromagnetic sense then an effective overall propagation constant along with the corresponding phase velocity for the composite mix can obtained as shown in equations 63 and 64:

$$\gamma_T = \gamma_s(1-\phi) + \gamma_w(\theta) + \gamma_A(\phi-\theta) = \alpha_T + j\beta_T \tag{63}$$

$$V_{P_T} = \frac{\omega}{\beta_T} \tag{64}$$

Where γ_T = Overall Propagation Constant of Soil Mix (3 phases)

γ_s = Overall Propagation Constant in Soil Solids

γ_w = Overall Propagation Constant in Water

γ_A = Overall Propagation Constant in Air

ϕ = Soil Porosity

θ = Soil Volumetric Water Content

α_T = Overall Attenuation Constant of Soil Mix (3 phases)

β_T = Overall Phase Constant of Soil Mix (3 phases)

V_{P_T} = Phase Velocity in Soil Mix (3 phases)

The overall propagation constants for the individual phases can be calculated using equations 27, 28, 29 and 34 for the water component and equation 34 for the solid and air components, entering the proper values for permittivity, permeability and conductivity.

Using equation 63 and 64 and solving for water content θ, an expression of the following form can be obtained:

$$\theta = K_1 + \frac{K_2}{V_{P_T}} \tag{65}$$

where K_1 and K_2 are constants that can either be empirically derived (linear regression on field data) or exactly derived from equations 27, 28, 29, 34, 43, 63 and 64. This is called the "index of refraction" equation, which relates water content directly to phase velocity (Herkelrath et al., 1991). K_2 is typically close to the phase velocity of waves in free space

and V_{p_T} is the effective phase velocity of the transmission line in an overall soil mix of the three phases as given by equation 64. The ratio of K_2 / V_{p_T} is called the index of refraction. Using equations 36, 63 and 64, an effective dielectric constant can be calculated as follows (assuming low conductivity):

$$\varepsilon_{eff} = \left(\frac{1}{V_{p_T}\sqrt{\mu_r \mu_0 \varepsilon_0}} \right)^2 \tag{66}$$

When the dielectric constant is properly determined, using equation 66, it can be used to determine the volumetric water content of the medium using calibration equations like the Topp equation shown in equation 26. Once the coefficients in equation 65 have been obtained, phase velocity values can be directly determined from field measurements using techniques such as TDR and those values entered into equation 65 to give water content. The key is accurately determining the dielectric constant or interpreting the phase velocity during the presence of excessive electrical conductivity and entering the proper values into either equation 26 or 65 to determine water content.

Intrinsic impedance and characteristic impedance of the transmission line in the composite mix can also be determined as follows:

$$\eta_T = \frac{j\omega\mu}{\gamma_T} \tag{67}$$

$$Z_T = \left(\frac{1}{\pi}\right) Cosh^{-1}\left(\frac{s}{d}\right)\eta_T \tag{68}$$

where

η_T = The intrinsic impedance in the overall composite mix

Z_T = The characteristic impedance of the parallel wire transmission line in free space.

The composite soil mix characteristic impedance (equation 68) along with the value for overall propagation constant in the composite soil mix (equation 63) can be combined with scattering (S) parameters and inverse fast Fourier transform (IFFT) algorithms to make accurate time domain predictions of TDR waveforms vs. water content and electrical conductivity and is the basis for the proposed TDR model.

3.6 Scattering (S) Parameter Theory

The Scattering or S-parameters are defined as follows for a 2-port network:

```
                 _____
            |                         |
    0-------|    2   Port    |--------0
Port 1      |                         |   Port 2
    0-------|    Network     |--------0
            |_____|
```
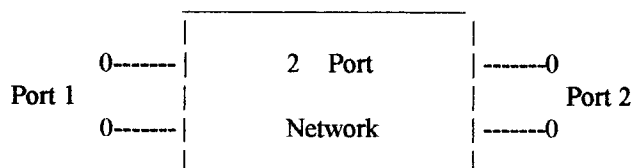
Scattering Coefficients (S-Parameters):

$$S11 \quad = \quad \frac{\text{Net Reflected Signal Level at port 1}}{\text{Incident Signal Level at port 1}} \quad \text{(with port 2 matched)} \quad (69)$$

$$S21 \quad = \quad \frac{\text{Net Transmitted Signal Level to port 2}}{\text{Incident Signal Level at port 1}} \quad \text{(with port 2 matched)} \quad (70)$$

$$S12 \quad = \quad \frac{\text{Net Transmitted Signal Level to port 1}}{\text{Incident Signal Level at port 2}} \quad \text{(with port 1 matched)} \quad (71)$$

$$S22 \quad = \quad \frac{\text{Net Reflected Signal Level at port 2}}{\text{Incident Signal Level at port 2}} \quad \text{(with port 1 matched)} \quad (72)$$

The two port network could be a series of cascaded two port networks in which only the last stage (input stage or output stage) is matched (load equals same impedance as last stage) to satisfy the above definitions. There could be several internal stages that are not matched leading to multiple reflections that add or subtract to form a composite reflected and transmitted signal. This is why the term "net" is in all the above definitions. An example of a cascaded network will be discussed later. The S-parameters can be also described by the following titles:

S11 = Input Net Reflection Coefficient

S21 = Forward Net Transmission Coefficient

S12 = Reverse Net Transmission Coefficient

S22 = Output Net Reflection Coefficient

3.6.1 S-Parameters of Simple Networks

For the case of a simple impedance boundary the S-parameters are given by:

```
0---------------0---------------0
               |
   Z1          |   Z2
               |
0---------------0---------------0
```
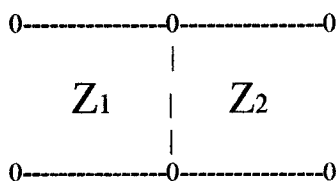
$$S11 \quad = \quad \Gamma_1 = \frac{Z_2 - Z_1}{Z_2 + Z_1} \quad = \quad \text{Input Reflection Coefficient} \tag{73}$$

$$S21 \quad = \quad \sqrt{\frac{Z_1}{Z_2}}(1 + \Gamma_1) \quad = \quad \text{Forward Transmission Coefficient} \tag{74}$$
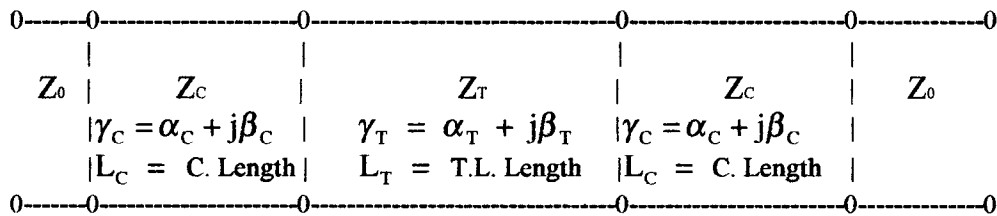
$$S12 \quad = \quad \sqrt{\frac{Z_2}{Z_1}}(1 + \Gamma_2) = \sqrt{\frac{Z_2}{Z_1}}(1 - \Gamma_1) = \text{Reverse Transmission Coefficient} \tag{75}$$

$$S22 \quad = \quad \Gamma_2 = \frac{Z_1 - Z_2}{Z_1 + Z_2} = -\Gamma_1 = \text{Output Reflection Coefficient} \tag{76}$$

Note that the S-parameters are normalized to impedance which satisfies conservation of energy.

3.6.2   S-Parameters of Cascaded Networks

Transmission Line with imperfect connectors attached to
cable with impedance = Z_0:

```
0------0--------------------0----------------------------------0----------------------0------------0
      |                    |                                  |                      |
  Z₀  |        Z_C         |              Z_T                 |        Z_C           |     Z₀
      |γ_C =α_C + jβ_C     |     γ_T  =  α_T + jβ_T            |γ_C =α_C + jβ_C      |
      |L_C  =  C. Length|     L_T  =  T.L. Length             |L_C  =  C. Length   |
0------0--------------------0----------------------------------0----------------------0------------0
```

Where

Z_T = Characteristic Impedance of Transmission Line

Z_C = Characteristic Impedance of Connectors

Z_0 = Characteristic Impedance of Coaxial Cable or Driving Line.

and

$\gamma_C = \alpha_C + j\beta_C$ = Overall Propagation Constant for the connectors.

$\gamma_T = \alpha_T + j\beta_T$ = Overall Propagation Constant for the transmission
line (equation 63).

and

Γ_C = Reflection coefficient between driving cable and connector.

Γ_T = Reflection coefficient between connector and transmission line.

L_C = Connector length

L_T = D.U.T. Transmission line length

If it is assumed first that a particular test fixture or device under test (D.U.T.) contains a transmission line (similar to that shown above) of some impedance (as defined by equation 57) and has wave propagation parameters (α and β) as defined by equations 35 and 36 and shown above, then it can be shown by two different methods (Transmission matrix generation and/or Mason's non-touching loop rule (Bailey, 1989; Helszajn, 1978) that the S parameter functions reduce to equations 77 and 78 if the device under test transmission line is terminated on both ends via ideal connectors ($\Gamma c = 0$, $\alpha c = 0$) to coaxial transmission lines of known impedance (say 50 ohms):

S-parameters for case of ideal connectors and 50 ohm termination on far end:

$$S11 = S22 = \frac{\Gamma\left(1 - e^{-2(\alpha + j\beta)z}\right)}{1 - \Gamma^2 e^{-2(\alpha + j\beta)z}} \tag{77}$$

and

$$S21 = S12 = \frac{\left(1 - \Gamma^2\right) e^{-(\alpha + j\beta)z}}{1 - \Gamma^2 e^{-2(\alpha + j\beta)z}} \tag{78}$$

where z equals the length of the device under test transmission line and α, β and Γ are as defined by equations 35, 36 and 62 respectively. Γ here equals the reflection coefficient between a boundary of 50 ohms and the device under test transmission line since the connectors are ideal and equal to 50 ohms in this case.

Equations 77 and 78 contain complex exponentials and so all these S-parameters can be further represented in terms of magnitude and phase components as follows:

$$S11_{mag} = S22_{mag} = \sqrt{\frac{\left[\Gamma\left(1 - e^{-2\alpha z} \cos(2\beta\ z)\right)\right]^2 + \left[\Gamma e^{-2\alpha z} \sin(2\beta\ z)\right]^2}{\left[1 - \Gamma^2 e^{-2\alpha z} \cos(2\beta\ z)\right]^2 + \left[\Gamma^2 e^{-2\alpha z} \sin(2\beta\ z)\right]^2}} \qquad (79)$$

$$S11_{phase} = S22_{phase} = \tan^{-1}\left(\frac{e^{-2\alpha z} \sin(2\beta\ z)}{1 - e^{-2\alpha z} \cos(2\beta\ z)}\right) - \tan^{-1}\left(\frac{\Gamma^2 e^{-2\alpha z} \sin(2\beta\ z)}{1 - \Gamma^2 e^{-2\alpha z} \cos(2\beta\ z)}\right) \qquad (80)$$

$$S21_{mag} = S12_{mag} = \frac{e^{-2\alpha z}\left(1 - \Gamma^2\right)}{\sqrt{\left[1 - e^{-2\alpha z}\Gamma^2 \cos(2\beta\ z)\right]^2 + \left[e^{-2\alpha z}\Gamma^2 \sin(2\beta\ z)\right]^2}} \qquad (81)$$

$$S21_{phase} = S12_{phase} = -\beta\ z - \tan^{-1}\left(\frac{e^{-2\alpha z}\Gamma^2 \sin(2\beta\ z)}{1 - e^{-2\alpha z}\Gamma^2 \cos(2\beta\ z)}\right) \qquad (82)$$

These models for S11 and S21 assume ideal connectors that are matched in impedance to the driving 50 ohm coaxial cables. In reality this assumption breaks down at a high enough microwave frequency where the electrical length of the connectors can no longer be neglected. More complete models for S11 and S21 which include connector effects are shown in equations 83 through 85. These expressions can again be derived by either Mason's non-touching loop rule or by multiplying cascaded transmission matrices for each subsection of the transmission line/connector complex and then mapping the T-parameters back into S-parameters (Anderson, 1967; Bailey, 1989; Helszajn, 1978; Hewlett-Packard, 1972). These models assume that the non-ideal behavior of the connectors are identical at both ends of the D.U.T. (i.e. a symmetrical cascaded series of networks).

S-Parameters with non-ideal connectors and 50 ohm termination on each end:

$$S11 = \frac{-e^{-2\gamma_T L_T}\left(e^{-2\gamma_c L_c} + \Gamma_c\Gamma_T\right)\left(\Gamma_C e^{-2\gamma_c L_c} + \Gamma_T\right) + \left(\Gamma_C\Gamma_T e^{-2\gamma_c L_c} + 1\right)\left(\Gamma_T e^{-2\gamma_c L_c} + \Gamma_C\right)}{-e^{-2\gamma_T L_T}\left(\Gamma_C e^{-2\gamma_c L_c} + \Gamma_T\right)^2 + \left(\Gamma_C\Gamma_T e^{-2\gamma_c L_c} + 1\right)^2}$$

$$= S22 \tag{83}$$

$$S21 = S12 = \frac{e^{-\gamma_T L_T} e^{-2\gamma_c L_c}\left(1-\Gamma_C^2\right)\left(1-\Gamma_T^2\right)}{-e^{-2\gamma_T L_T}\left(\Gamma_C e^{-2\gamma_c L_c} + \Gamma_T\right)^2 + \left(\Gamma_C\Gamma_T e^{-2\gamma_c L_c} + 1\right)^2} \tag{84}$$

where $\gamma_C = \alpha_C + j\beta_C$ = Overall Propagation Constant for the connectors.

$\gamma_T = \alpha_T + j\beta_T$ = Overall Propagation Constant for the transmission line.
as defined by equation 63.

and

Γ_C = Reflection coefficient between driving cable (50 ohms) and connector.

Γ_T = Reflection coefficient between connector and transmission line D.U.T.
as defined by equations 57 and 62.

L_C = Connector length

L_T = D.U.T. Transmission line length

By setting Γ_C and γ_C equal to zero (ideal connectors) equations 83 and 84 reduce to 77 and 78.

For the case of an open circuit termination at the far end of the transmission line the expression for S11 becomes that shown in equation 85:

Open circuit termination at far end of transmission line:

(i.e. TDR Probe):

$$S11 = \frac{e^{-2\gamma_T L_T}(e^{-2\gamma_c L_c} + \Gamma_c \Gamma_T)(e^{-2\gamma_c L_c} - \Gamma_T) + (-\Gamma_T e^{-2\gamma_c L_c} + 1)(\Gamma_T e^{-2\gamma_c L_c} + \Gamma_C)}{e^{-2\gamma_T L_T}(\Gamma_C e^{-2\gamma_c L_c} + \Gamma_T)(e^{-2\gamma_c L_c} - \Gamma_T) + (\Gamma_C \Gamma_T e^{-2\gamma_c L_c} + 1)(-\Gamma_T e^{-2\gamma_c L_c} + 1)} \quad (85)$$

Even more complete models for predicting S11 and S21 can be developed from Mason's Non-Touching Loop Rule to accommodate even more cascaded stages. These more complete algorithms are the basis of the computer models proposed in this research. As can be seen these expressions are functions of the parameters: α (attenuation constant), β (phase constant), Γ (reflection coefficient) and z (probe or transmission line length or connector length) for each of the cascaded stages and boundaries (i.e. connectors, device under test transmission line, etc.). By examining equations 27 through 68 it is seen that the S-parameters are therefore ultimately functions of frequency as well as the basic parameters ε (electric permittivity), μ (magnetic permeability), σ (electrical conductivity) and finally probe geometry. The electric permittivity ε is itself a complex function of frequency and other parameters as described by equations 27 through 29 especially in the case of water. The electrical conductivity σ is considered a DC variable and is not treated as a function of frequency in these models. The magnetic permeability μ is considered a constant and equal to that of free space (1.26E-6 Henries/meter) in this thesis.

The theories of electromagnetics and S-parameters and their associated models will form the basis of the proposed TDR soil water content and electrical conductivity measurement prediction model or algorithm.

3.7 Nuclear Magnetic Resonance (NMR): Theoretical Basis

Quantum mechanics is a branch of physics stating that matter is composed of particles that exist at discrete energy levels only. When combined with electromagnetics this gives rise to a soil moisture measurement technique known as nuclear magnetic resonance or NMR. This technique offers promise as a non-invasive soil water content and water potential measuring device in the upper portions of the soil and so is discussed in this section along with the background theory of quantum mechanics. Ongoing research is warranted but will be left to other researchers.

Examples of the discrete energy levels described by quantum mechanics include the energy levels of electrons in an atom or molecule as well as the energy levels associated with spin states of the atomic nuclei. In the theory of quantum mechanics electromagnetic waves are said to possess discrete packets of energy dependent on their frequency based on the following relationship (Gadian, 1982):

$$\Delta E = Energy = h\nu \tag{86}$$

where

h = Planck's constant = 6.626E-34 JouleSeconds

ν = frequency (Hz).

This says that energy from electromagnetic radiation at the right frequency can be adsorbed by certain atoms or molecules by having their electrons (or alternatively the spin of the nuclei) jump in energy level by the amount predicted by equation 86. If the energy jump is to a valid quantum state then the electromagnetic radiation energy will be adsorbed. This is termed resonance and it will be shown that there are several different types of resonance's and thus quantum states or types. The inverse is also true: if an electron drops in energy level to the next lower state then electromagnetic radiation will be emitted at a certain frequency as predicted from equation 86.

Some examples of quantum energy transitions are shown below with the corresponding frequency range of emission (or adsorption).

1.) Change in energy states of inner
   electrons of atoms or molecules: X-ray frequency range

2.) Change in energy states of outer or
   valence electrons: Visible and Ultraviolet frequency range.

3.) Molecular rotational & vibrational
   energy transitions (thermal effects):   Microwave and Infrared frequency range.

4.) Transitions between closely spaced
   energy levels such as magnetic states
   of atomic nuclei: Radio Frequency range (1 to 500 MHz).

Examples of phenomena that can emit the above various frequencies are shown below:

1.) X-Rays: Energy imparted by colliding electrons that have been accelerated
                   by very large electric fields for example those accelerated by high
                   voltages (>15KV) in tubes or arcing high voltage relays with small
                   gaps between their contacts.

2.) Visible & UV: Semiconductor light emitting diodes (LEDs), ionizing gases &
                   arcing when the electric fields aren't as high (still could be
                   higher voltages but over longer distances or gaps). Extremely
                   high temperatures.

3.) Infrared: Thermal effects such as body heat, respiration, soil heat, etc.

4.) Radio Frequency
   (RF: 1-500MHz): Nuclear Magnetic Resonance (NMR)

There are several types of quantum states. Some examples are given below for electrons and then for nuclei.

Electron quantum numbers:

Type	Symbol	Possible values	Quantity determined
1. Principal (electrons)	n	1,2,3,.....	Electron Energy
2. Orbital	l	0,1,2,...n-1	Magnitude of Angular Momentum
3. Magnetic	m_l	$-l$ .... $+l$	Direction of Angular Momentum
4. Spin Magnetic	m_s	$-1/2$ or $+1/2$	Direction of Electron Spin

Protons and neutrons in the nucleus also have quantum states such as spin and angular momentum and are usually coupled together to give a quantum state for the nucleus. One such type is nuclear spin I which can have values of the following (Gadian, 1982):

$I = 0$ for nuclei with even numbers of both neutrons and protons.

$I = 1/2, 3/2, 5/2, 7/2$, etc. (half integral) for nuclei with odd mass numbers.

$I = 1, 2$, etc. (integral) for nuclei with even mass number.

Another quantum state in the nucleus is nuclear angular momentum vector (orientation or direction) and is designated m and can have any of the following $(2I + 1)$ values:

$$m = I, I-1, ... -I$$

These discrete quantum states correspond to energy levels that are given by the following:

$$E = -\mu_z B_o \tag{87}$$

where

μ_z = magnetic moment (not to be confused with magnetic permeability).

B_o = external magnetic flux density (Tesla)

Combining equations 86 and 87 along with nuclear quantum numbers:

$$E = \frac{-\gamma\, h\, m\, B_0}{2\pi} \tag{88}$$

where

γ = gyro magnetic or magnetogyric ratio of the nucleus.

m = nuclear angular momentum vector quantum number.

If the nuclear spin quantum number I = 1/2 (such as in hydrogen H) then m can be either + 1/2 or -1/2. It can then be shown that a transition between these two quantum states results in a energy transition of the following:

$$\Delta E = \frac{h\gamma\, B_0}{2\pi} \tag{89}$$

Also remembering from the quantum mechanics of electromagnetic waves that energy is related to frequency (equation 86), an expression can be derived for the resonant frequency v_o that can cause a transition between these two nuclear quantum states:

$$v_0 = \frac{\gamma\, B_0}{2\pi} \tag{90}$$

This is termed the nuclear magnetic resonance frequency and is the basis of another technique to measure soil water content and possibly soil water potential. This is due to the fact that hydrogen is especially visible using this technique and it is obviously a constituent of water.

NMR measurements are conducted in the following manner: A large external magnetic field (of flux density = B_o = 0.1 to 6 Tesla range) is aligned across a sample of soil (oriented in the z direction for this analysis). Then an electromagnetic wave of frequency equal to that determined by equation 90 is sent in orthogonal to the magnetic field (i.e. in the xy plane) so that the nuclear angular momentum vector can be tilted away from equilibrium by a certain angle. If the RF signal is on long enough then the nuclear angular momentum vector can be tilted to an angle 90° out of phase with equilibrium or into the xy plane. When the RF signal is turned off the nuclear angular momentum vector will "relax" back to equilibrium. During this relaxation process energy will be released in the form of an electromagnetic wave at the same nuclear magnetic resonance frequency as given by equation 90 (Abraham et al., 1988; Harris, 1986).

There are two different relaxation times termed T1 and T2. T1 is termed the spin-lattice relaxation time and it is the time constant associated with the return to equilibrium of M to Mz (equilibrium angular momentum vector). This transition is therefore modeled by the following first order exponential transition:

$$\frac{d\,Mz}{dt} = \frac{M_0 - Mz}{T1} \tag{91}$$

The spin-lattice relaxation process is due to the exchange of energy between the nuclear spins and the molecular framework.

T2 is termed the spin-spin relaxation time and is the time constant associated with the relaxation of the xy component of the angular momentum (i.e. Mxy) back to its

equilibrium value of zero. It is also modeled by a first order exponential by the following equation:

$$\frac{d\,Mxy}{dt} = \frac{-Mxy}{T2} \tag{92}$$

Spin-Spin relaxation involves interactions between neighboring nuclear spins without any exchange of energy with the molecular lattice. These two relaxation times can be measured or determined by how fast the radiated RF (at the NMR frequency) is detected by external instrumentation. There are two peaks, or RF bursts, which are detected at different times and which correspond to the two distinct relaxation processes.

Since there are two separate angular momentum direction quantum numbers, m, which are possible for hydrogen ($+1/2$ and $-1/2$) there is some probability that there will be a population of nuclei at each quantum number. If n- is the population of nuclei at $m = -1/2$ (higher energy state) and n+ is the population of nuclei at $m = + 1/2$ then the relative populations between them can be predicted by a Boltzmann Distribution as follows:

$$n\text{-} \,/\, n\text{+} = \exp\left(-\Delta E \,/\, kT\right)$$
$$= \exp\left(-h\,\gamma\,B_o \,/\, 2\pi kT\right) \tag{93}$$

where k = Boltzmann constant.

At thermal equilibrium this ratio is very close to unity (slightly less) and so typical values of ΔE are very small. If the externally applied magnetic flux density was zero ($B_o = 0$) then the populations would be equal. When more energy is added (i.e. larger external flux density) then n- changes in number relative to n+ in the material. For NMR to work there needs to be a difference in these two populations so that the orthogonal oscillating magnetic field component of the incident electromagnetic wave (B1 in the xy plane at the

NMR frequency) can couple energy to the system to tilt the magnetic moment vector out of its equilibrium position. Therefore B_o needs to be as large as possible to allow for more nuclei to be able to adsorb this energy. This low ΔE (even for large values of B_o) causes the resonant frequency to be low (in the RF range: 1 to 500MHz) due to the small energy differences between the two quantum states. Also since the populations of nuclei at the higher state are only slightly less than those of the lower state only a small amount of net energy is adsorbed when the orthogonal resonant frequency wave is applied. This causes an inherent lack of sensitivity in the NMR method and therefore the radiated signals during relaxation are usually at a very low level greatly limiting the depth to which these signals can be detected from out of a test medium.

Since the levels of signals are so small a newer technique called pulsed Fourier transform NMR is the preferred method of obtaining NMR information. In this technique a pulse or burst (short duration - typically microseconds) of RF is sent into the test medium to provide the orthogonal oscillating magnetic field B1. The Fourier transform of this pulse is such that all the resonant frequencies of interest are contained in it. For example, it is possible to image phosphorus, hydrogen and carbon all at the same time with this technique (frequency components at all their resonance's would be superimposed on each other). The radiated signal during relaxation would then be a complex composite of all these resonances occurring at their respective relaxation times. Modern signal processing hardware and software can easily perform a Fourier transform on this composite signal separating out all the desired information. This composite signal will also be at a larger amplitude than if a single frequency was used allowing it to be more easily detected. The overall signal amplitude is still not very high and so an additional step of taking multiple readings and adding them to each other will improve the signal to noise ratio. This is because adding uncorrelated noise is proportional to the square root of the number of readings whereas adding the composite NMR signal to itself is directly proportional to the number of readings. Therefore the signal to noise ratio will improve by the square root of the number of readings. This means that more readings will be required to detect smaller signals which slows down the measurement.

Another approach to the NMR method is called "spin echo" where two orthogonal pulses are applied to the medium (one at a duration that causes a 90 degree tilt and one that causes a 180 degree tilt from the equilibrium position). The 90 degree pulse is sent out first and then the 180 degree pulse follows. This refocuses some of the dephasing that goes on during spin-spin relaxation (T2 processes) and makes it easier to measure or determine T2.

Matzkanin and Paetzold (1982) showed that soil moisture content affects T2 and therefore determination or measurement of this spin-spin relaxation time can be used to help determine soil moisture content. Tollner et al. in 1987 showed that water content can be correlated to a particular coefficient of a regression equation involving T2 but not exactly to T2 itself. Nevertheless, Tollner et al. (1987) still showed that soil water content can be determined by NMR. Tollner et al. (1987) also hypothesized that T2 may be correlated to water potential stating that the amount of energy required to remove water from a location may somehow effect the length of T2. More research is needed to test this hypothesis but if it proved true then the first true non-invasive method of measuring water-potential in a soil would exist.

There are a number of limitations to NMR when it comes to measurements in the soil. The first is the difficulty of maintaining a uniform external magnetic flux density (B_o) in the soil. Equation 90 shows that the nuclear magnetic resonance frequency is dependent on B_o and so if that external magnetic field isn't homogeneous or constant then the NMR signal for hydrogen will be almost impossible to signature out of a test sample or soil sample. This is due to the fact that hydrogen already has several resonances due to chemical shifts associated with different hydrogen-containing compounds many of which may be in the soil (especially if organic matter content is high). Non uniformity in the magnetic field will jumble all these resonances in much the same manner as shuffling a deck of cards turning the process into a software and signal processing nightmare to get the desired information. Therefore the NMR water content measurement technique is

limited to the top few inches of the soil if it is desired to keep the measurement non-invasive while maintaining accuracy. George A. Matzkanin of the Southwest Research Center showed that such a field measurement device can be made and be pulled behind a tractor (Hogan, 1986). His device was able to measure water content to depths of 2.5 inches. This device originally had magnet pole pieces that extended some 4.5 inches into the ground and so furrows or trenches had to be made for them via disks. It was later modified to be a truly non-invasive device. Paetzold et al. in 1987 compared the results of using the invasive vs. non-invasive field NMR instruments with the conclusion being that both will work but the non-invasive version will have slightly lower sensitivity due to not maintaining the magnetic field uniformity over as great a depth. More research needs to be conducted in this area to see if the depth of measurement can be increased.

Another limitation to this method comes when there are ferromagnetic materials in the soil (Rogers et al., 1987). This will alter any externally applied magnetic field and therefore shift the NMR frequency of hydrogen or any other element of which an attempt is being made to detect. Typically, however, the external magnetic field flux density is very large and will not be greatly altered by local magnetic materials in the soil unless they are in great concentration. Finally another, and possibly greater, limitation to NMR is that since their emitted RF signals are at a very low level they can be quickly attenuated into the noise floor by conductive soils and so NMR would probably not work very well at significant depths in conductive soils. Also heterogeneity in the soil may scatter some of the RF signals but this could be used to advantage with powerful signal processing software to make an image of the soil beneath the magnet, but too much heterogeneity may be impossible to interpret.

One very important ray of hope is that organic matter content and other soil characteristics, as well as its heterogeneity, are probably relatively constant over time at depths below say a few feet. If NMR could be modified to be able to scan at those depths then the heterogeneity and other factors could be averaged out over time in multiple readings with the water content being the only variable. In these types of conditions absolute numbers might not mean much but relative images from day to day possibly could

be correlated to water content changes. Also at depths near the surface where soil conditions change more rapidly, NMR could possibly be used to discern some of these changes with proper signal processing software. Often the water component of hydrogen is large compared to other compounds and the heterogeneity of the soil might not matter anyway. NMR could possibly be used to determine the soil structure, particle size distribution, and porosity (Hinedi et al., 1993; Hinedi et al., 1995) and perhaps information about organic matter content, as well as nitrogen (N), Phosphorus (P), Potassium (K), and Carbon (C) contents since it is able to signature out several different elements and compounds. NMR has been demonstrated to show promise in imaging many of the physical and chemical properties of porous rocks (Vinegar, 1986) as well as plant roots (Rogers et al., 1987). Much more research is warranted for NMR.

4. SUMMARY & SELECTION OF RESEARCH FOCUS

There are many different indirect methods of determining volumetric water content, water potential, as well as the location of water in the soil. Geophysical, Thermal, Radioactive and Electromagnetic (including quantum mechanic) methods exist and all have their own advantages and disadvantages and therefore warrant more research. Electromagnetic methods offer great promise in measuring the soil moisture properties with a minimum amount of soil disturbance, maximum accuracy and resolution, high measurement speed and automation with a minimum amount of calibration.

Electric field methods include soil resistance and soil capacitance sensors as well as resistance of devices in equilibrium with the soil water. All of these methods offer simplicity but rely on models of the soil electrical properties that are relatively simplistic and don't necessarily account for bulk electrical conductivity and frequency dependent dielectric variations in the soil.

Magnetic field methods include induced fields as well as detection of fluctuations in the Earth's magnetic field. These methods are all non-invasive and relatively simple to use. The induced field methods are again vulnerable to other sources of dc conductivity such as variance in the salinity of the water as well as other conductive materials in the soil effecting the location and magnitude of induced current loops in the soil. Fluctuations of the Earth's magnetic field might be caused by other magnetic materials and it may be difficult to signature out water which by itself is slightly diamagnetic and therefore largely non-magnetic. Water pockets may create regions of lower magnetic permeability relative to the surroundings (if they contain magnetic solids such as iron) and this possibly could be detected by sensitive instrumentation but it is unlikely that this would lead to the accurate determination of water content.

Propagating electromagnetic waves can be used to determine many properties of the soil such as the location of water at various depths (ground penetrating radar GPR) and determination of the amount of water or water content in the soil (GPR, TDR and microwave remote sensing). GPR is a true non-invasive measurement technique. With suitable computing and signal processing power GPR could be used to measure water content and electrical conductivity in the soil and so this method is deserving of more research. Microwave remote sensing is also a non-invasive method and is good for making field scale measurements and estimates of soil water content near the surface of the soil. Great difficulty can occur in accurately interpreting the remote sensing data and the method is dependent on good weather and the availability of airplanes or satellites. TDR is used to measure the dielectric constant of the soil (or the phase velocity of the wave) and correlate that to water content. For non-conductive, non-magnetic soils TDR, in its present form, is a viable measure of soil moisture content. TDR offers promise as an accurate measurement technique of both water content and electrical conductivity (or salinity) even if salinity is high if the proposed wave propagation models are used in its calibration algorithms. TDR also shows promise as a potentially non-invasive water content measurement tool at the soil surface if air gaps are minimized (Selker et al., 1993; Flugstad, 1995). TDR responds quickly to changes in soil moisture due to its fast measurement time and can be easily incorporated into automated test systems. The disadvantages of the propagating wave methods (GPR, TDR and Microwave remote sensing) include the following: Propagating electromagnetic waves can be greatly attenuated by soil electrical conductivity and the imaginary component of complex permittivity (especially at higher frequencies). These waves can be reflected and refracted by discontinuities in the intrinsic impedance of the soil. This can cause both scattering and rapid jumbling of the signals if the soil heterogeneity is great. If the soil electrical conductivity and/or imaginary component of the complex permittivity is high the phase velocity will no longer be solely dependent on the dielectric constant but instead on the conductivity, complex permittivity and frequency (where the loss tangent is greater than one). Ferromagnetic materials in the soil can also affect the phase velocity of an electromagnetic wave. These disadvantages could be overcome by using more complete

models and the efficacy of these proposed models will be tested in the research to follow using a TDR system but could be employed in a GPR or remote sensing system as well.

Quantum Mechanic approaches can be used to measure soil moisture as well. Studies by Tollner et al. (1987), Matzkanin & Paetzold (1982), Paetzold et al. (1987) as well as Matzkanin's field instrument (Hogan, 1986) have demonstrated that Nuclear Magnetic Resonance can be used to measure soil water content by correlating it to the spin-spin relaxation time T2 or to coefficients of regression equations involving T2. In addition, Tollner et al., in 1987 hypothesized that soil water potential may correlate to T2 or other NMR parameters. NMR has been demonstrated to be a viable non-invasive field measurement tool for soil water content to depths of 2.5 inches in the soil (Hogan, 1986). The limited sensitivity of NMR as well as the dependence on large externally applied and homogeneous magnetic fields may make it unfeasible for use in measuring soil water parameters at depths greater than say a foot or more. More research is needed in this area.

Possible combinations of all the above methods may be used to get information on the soil water conditions. Improved digital signal processing software and better data acquisition hardware and computing capabilities is making it more feasible to extract meaningful information out of jumbled signals from the soil that can come with electromagnetic methods. There is good potential for creating non-invasive soil moisture probes using electromagnetic methods. At the present time, time domain reflectometry, (TDR) probably offers the greatest balance of all the issues of measurement accuracy, resolution, suitable imaging volume, speed, response time to changing soil conditions, potential for reduced soil disturbance, reduced calibration, automated data acquisition and the ability to measure both water content and electrical conductivity (or salinity) and so is the basis of the proposed research project to follow. A lower cost (reduced frequency range), lower calibration requirement, less-invasive field grade TDR water content and electrical conductivity (or salinity) measurement system will be the goal of this ongoing research. The cost of measurement is presently fairly high with TDR but might be reduced by using only relevant frequency ranges with the TDR system (Flugstad and Selker, 1996).

5. LITERATURE REVIEW ON TDR SALINITY PROBLEMS

Over 100 articles have been published concerning the application of Time Domain Reflectometry to the measurement of volumetric soil water content since 1980. In this thesis attention is restricted to research directly related to TDR in saline environments or in regions of high electrical conductivity (low frequency conductivity due to solutes in solution) as well as in regions of high complex permittivity due to polar molecule self resonances (i.e. water at microwave frequencies or organics at RF frequencies).

Dalton et al. in 1984 and 1986 and Dasberg and Dalton in 1985 showed that TDR can be used to simultaneously measure water content and bulk electrical conductivity by measuring the attenuation or dissipation of the traveling wave over the distance of the probe and using the expressions of attenuation constant as a function of frequency and conductivity from classical electromagnetic theory.

Arcone (1986) concluded that electrical conductivity can cause problems in single reflection TDR measurements due to false dispersions resulting from the incomplete decay of the TDR waveform. He concluded that finite conductivity values can give the impression of dielectric dispersion where there is none. He gave several guidelines for the recognition of when conductivity is present and can cause errors. He concluded that for single reflection TDR that the conductivity should be below 0.1 dS/m for relaxation frequencies above 1 GHz.

Topp et al. in 1988 noted that in soils, the imaginary part of the dielectric constant as well as attenuation, was not negligible and its frequency dependence should be investigated to better understand its contribution to TDR conductivity measurements.

Zegelin et al. in 1989 investigated using a multiwire symmetric probe to emulate a coaxial cable to provide a better match at the coaxial cable-probe interface to minimize

errors due to reflections at that interface. They concluded that electrical conductivity measurements could be made within 10% if the conductivity exceeded 0.1dS/m.

Bertolini et al. in 1990 demonstrated that TDR can be used to study the dielectric properties of liquids by measuring the real and imaginary components of the electric permittivity vs. frequency and therefore characterizing their polar resonance frequency. They claimed to be able to measure these parameters up to 7 to 10 GHz with good accuracy as long as spurious reflections were accounted for as well as fringing fields at the open circuit termination.

Campbell (1990) studied the dielectric properties and influences of conductivity in soils over the frequency interval of 1 to 50 MHz. He concluded that at lower frequencies the real dielectric behavior becomes complicated by ionic conductivity. He stated that the imaginary component of the dielectric constant is variable over soil type due to a loss mechanism that varies greatly with soil salinity. He also concluded that ionic conductivity in soil pore water is able to explain the dispersion present over the frequency interval of 1 to 50 MHz.

Van Loon et al. in 1990 proposed a new method of measuring bulk electrical conductivity in soils by comparing TDR reflections in the soil to a reference in air. The intent was to remove all uncertainties caused by the measurement system and to allow the measurement system to only look at the differences between the medium and air. They used the attenuation of the second reflection in their calculation of bulk conductivity.

Dalton et al. in 1990 and Dalton in 1992 noted that in conditions of high electrical conductivity, where the pore water salinity is greater than 8 dS/m, that an overestimation of water content is possible due to errors caused possibly by the dispersive behavior of the propagating electromagnetic pulse.

Nadler et al. in 1991 demonstrated a new method of measuring the electrical conductivity directly by measuring the transmission line characteristic impedance using the first reflection information from TDR. Their results were found to correlate well with four-electrode measurements. They stated this method was more accurate than measuring the attenuation of the signal from the second reflection due to other multiple reflection sources which can further attenuate the returning signal in a second reflection measurement causing errors in the determination of electrical conductivity.

Kelly et al. in 1996 investigated wrapping the conductors of a parallel wire transmission line with a thin layer of Teflon heat shrink tubing. They concluded that soil water content measurements could be made in soils with high salinity by using such a probe, although a separate calibration curve is required.

Heimovaara et al. in 1994 discussed the benefits of performing frequency domain analysis on TDR waveforms to understand better the contribution of the complex electric permittivity in affecting water content and bulk soil electrical conductivity measurement accuracy. They proposed a four component dielectric mixing model (air, solids, bound water and free water) for soils based on the volumetric mixing of the refractive indices of the individual components. Their analysis concentrated on frequencies below 150 MHz.

To date no author has presented a rigorous mathematical model to describe the behavior of TDR wave propagation in conductive media over the entire range of frequencies important to TDR (mainly 100 MHz $< f <$ 10 GHz) that accounts for both the real and imaginary components of the electric permittivity in influencing the shape of TDR waveforms and combines that with the complexities of real TDR probes that contain non-ideal connectors and boundaries using S-parameter network theory.

6. PROPOSED TIME DOMAIN REFLECTOMETRY (TDR) MODEL

6.1 TDR Background Theory

Time Domain Reflectometry (TDR) is a soil water content (and potentially salinity) measurement technique that is based on the accurate interpretation of electromagnetic wave propagation down a transmission line probe inserted into a soil. TDR instrumentation makes use of a high frequency step generator, microwave sampling oscilloscope and a coaxial cable connection to a measurement probe, which consists of an open circuit terminated transmission line that may be two parallel wires (or other types).

The rise time of the step or pulse is typically around 250 picoseconds and may be as fast as 30 picoseconds. The pulsewidth is usually wide compared to the risetime, typically from 10 nanoseconds to 25 microseconds in duration. Therefore, the waveform is usually thought of as a step, whose Fourier transform would include two groups of frequency components separated by several decades on a log frequency scale. One group of components is up in the microwave range (1 to 20 GHz), with the fundamental frequency reflecting the risetime of the step. The other frequency group is in the 10 kHz to 100 MHz range with a fundamental frequency dependent on the pulse width of the step. A Fourier analysis would also yield a DC component affected by the amplitude of the step.

The TDR step waveform or pulse is sent down a coaxial cable of impedance typically close to 50 ohms. The waveform then reaches the probe, which might consist of a short parallel wire transmission line inserted into the medium being tested. The parallel wire transmission line is open circuited at its far end. The waveform will be partially reflected at the coax-probe interface, due to a mismatch in impedance with the probe, and this is called the first reflection. The reflection at the far end of the probe (open-circuit termination) is called the second reflection.

The phase velocity of the propagating wave can be determined from the length of the transmission line divided by the length of time it takes the propagating wave to traverse the transmission line. As can be seen from equation 43, if σ is zero and the imaginary component of the complex permittivity is zero (i.e. perfect insulator), then the phase velocity of a wave is independent of frequency and is inversely dependent on the square root of both the magnetic permeability μ and electric permittivity ε. It was shown earlier that μ does not vary much from dry soils to wet soils since pure water has no ferromagnetic properties. This means that in a soil with very low conductivity only ε varies appreciably with changing soil water content. Therefore a measure of the transit time (and therefore phase velocity) of a traveling wave can be used to determine the dielectric constant from equation 43 or 66 with that value then plugged into equation 26 (Topp equation) to obtain water content θ. The phase velocity value can also be used directly to determine water content using equation 65 (index of refraction equation) and this is considered the preferred method at this time.

6.2   TDR Problems

A key assumption of TDR in its present implementation is that the soil electrical conductivity is low. This is not true in saline water conditions or in soils with significant amounts of metals in them. It was shown that in the presence of electrical conductivity, dispersion between the low frequency groups and high frequency groups of the step waveform may occur (equations 43, 51 and 52). Also, the high frequency components may be attenuated relative to the low frequency components. Finally, the low frequency components may be reflected at the first reflection in a different fashion than the high frequency components. All these factors can cause errors in the determination of dielectric constant and therefore water content. In general, most soils have low conductivity but in arid regions the soil is often more conductive especially if low quality irrigation water is used and so care must be taken when using TDR. Another assumption of TDR, which holds for most soils, is that $\mu = \mu_o$ or that the relative magnetic permeability $= 1$.

6.3 Proposed Model

The proposed models for predicting TDR water content and electrical conductivity measurements are based on S-parameter network theory as well as on electromagnetic theory. They make use of the S-parameter expressions for cascaded networks given by equations 83-85 or Mason's non-touching loop rule for more complicated networks, and combine them with electromagnetic wave propagation and reflection equations as well as transmission line equations given by equations 27-29, 34-36, 39-41, and 43-68 to develop the models to predict the S-parameter results. Mixing models accounting for the three phases of water, air and solids are included in the overall models. The effects of non-ideal connectors and fixture boundaries can also be included in these models. These models give predictions of the S-parameters vs. frequency. To get a time domain prediction or predict a TDR waveform shape, equation 85 is used together with an Inverse Fast Fourier Transform (IFFT) algorithm over a harmonically related set of frequency points.

6.4 Model Predictions

Some preliminary predictions of TDR performance using the proposed models in their present state were made by incorporating the mathematical models into MathCAD (complex equations) and Lotus 123 (tabulations, graphs and some of the math). Predicted results (time domain) for the following conditions (assuming nearly-ideal connectors and boundaries) are shown in figure 6:

Transmission Line Type:	Invasive parallel wires of 7.5 cm length.
Soil Type:	Sand
Water Content:	0 (dry soil) and 0.36 (wet soil)
Effective Dielectric Constant:	2.7 (dry soil) and 20 (wet soil)
Bulk Soil Electrical Conductivity:	0 dS/m, 1 dS/m and 10 dS/m
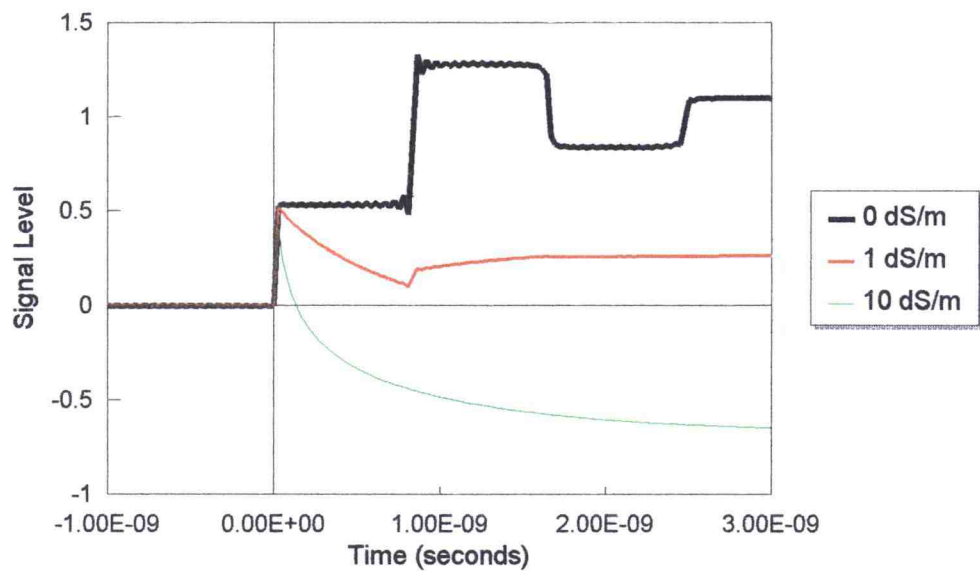
a.)
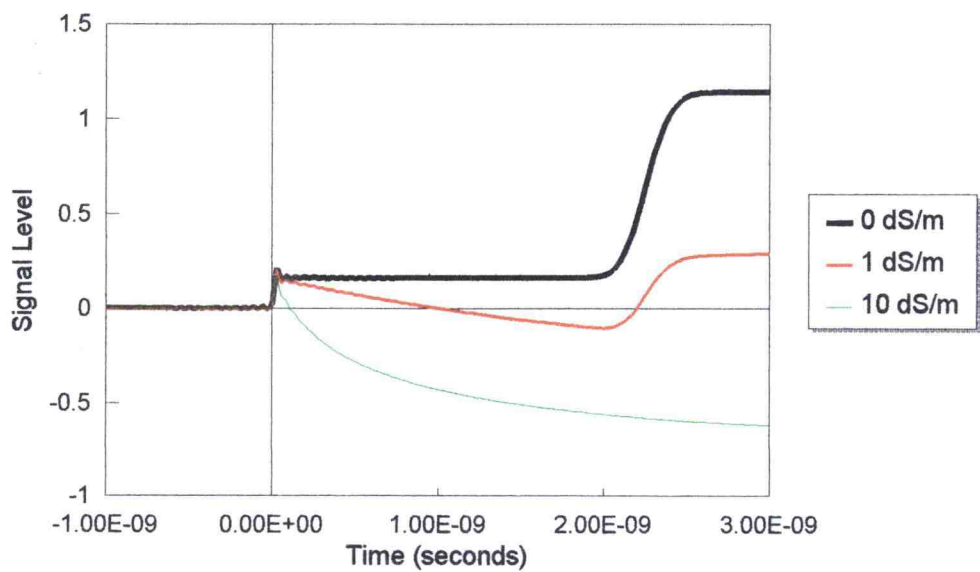
b.)

Figure 6. Time domain predictions vs. electrical conductivity for a.) dry soil ($\varepsilon_r = 2.7$) and b.) wet soil ($\varepsilon_r = 20$) conditions.

The predictions for the non-saline cases show the dependence on water content of the transit time (time between detection of first and second reflections) as well as the reflected levels as predicted by equations 43, 57 and 62.

The predictions for the saline cases show the affects of attenuation, dispersion and frequency dependent reflections. The second reflection is nearly invisible in the more saline cases due to excessive attenuation of the high frequency components of the signal returning on the transmission line. In the saline cases the trace droops down gradually and goes negative due to low frequency dispersion as well as lower impedances at low frequencies (resulting in negative reflection coefficients on the low frequency components) as predicted by equations 52, 58 and 62.

Finally, even in the non-saline conditions, for the wet soil case there is evidence of some attenuation and dispersion on the high frequency components of the second reflection due to the complex permittivity of water given by equations 27 through 29 and accounted for in equations 43, 57 and 62. This is evidenced by the lack of sharpness on the second reflection.

7. MATERIALS AND METHODS FOR VALIDATING THE MODEL

A comprehensive validation of the proposed TDR models to predict water content and electrical conductivity measurement performance is currently under way and those results along with fully refined models to give a best "fit" to the data will be given in the Ph.D. dissertation that will follow the proposed ongoing research project. Also given in the Ph.D. dissertation will be answers to the fundamental research question of whether or not these models can be used in a field grade TDR water content and electrical conductivity measurement system to achieve the desired design goals.

In this Master's thesis, predictions will be given of TDR performance using the models in their present state, and some of the early preliminary results are given that compare the predictions to actual data in real systems. These early results help give confidence in the models but will also be used to help expose remaining problem areas or questions that can be answered in the Ph.D. portion of the research.

The basic methodology of these experiments is to compare the predictive models to actual measured results of the propagation characteristics of electromagnetic waves in media that emulate both saline and non-saline soils. These parameters include reflection at media boundaries, attenuation across the medium and travel time or phase velocity through that medium. These parameters are all obtainable from the S-parameters that characterize a particular network, such as a parallel conductor transmission line, which were defined by equations 69 - 85 for various complexities of networks as well as types of terminations. The predictive models make use of equations 83 - 85 or Mason's Non-Touching loop rule for more complicated networks and combine them with equations 27-29, 34-36, 39-41, and 43-68 to develop the models to predict the S-parameter results. The effects of non-ideal connectors and fixture boundaries are included in the models. These predictions will be compared to actual measured results of the S-parameters which are obtained using a Hewlett Packard HP8510 network analyzer equipped with an S-

parameter test set. All of these measured S-parameters have both a magnitude and a phase component and are a function of frequency and so network analysis is a swept frequency type of measurement. The predictions will be compared to the actual measured results in the frequency domain (looking at the magnitude component) for cases of a 50 ohm load at the end of the transmission line (S11 and S21) as well as an open circuit at the far end (S11 only). Time domain comparisons will also be made by performing an Inverse Fast Fourier Transform (IFFT) on both the predicted and actual measured results for S11 (magnitude and phase) with the transmission line open circuited to emulate a TDR probe.

In these experiments both invasive and non-invasive probes are being used. The invasive probes are parallel wire transmission lines and the non-invasive probes are circuit board mounted parallel trace transmission lines. Two different types of non-invasive probes are being tested: A 3-conductor unbalanced parallel trace (coplanar microstrip) pattern and a 2 conductor parallel trace (balanced microstrip) pattern. The non-invasive circuit boards were placed on both the top and bottom of the test fixtures to test for uniformity of water content in the fixture, and the effects of air gaps at the top and water films at the bottom.

Four test fixtures are being used, each containing one invasive transmission line through the middle of the fixture and two non-invasive circuit boards (with a transmission line microstrip pattern etched on them) mounted on the top and bottom of the fixtures. Each fixture contains an equivalent volume of a 40/50 grade of sand (Unimin/Accusand). The fixtures are cylindrical in shape with an inside diameter of 3" (7.62 cm) and a height of 1"(2.54cm) giving a volume of 115.83 cm^3. Volumetric water content θ, one of the independent variables (defined by equation 1), is given as follows for these test conditions:

$$\theta = \frac{\text{Volume of Water}}{\text{Total Fixture Volume}} = \frac{(\text{Mass of Wet Soil - Mass of Dry Soil})}{(115.83 \text{ cubic cm})(1 \text{ g H}_2\text{O / cc})}$$

Both ends of the test fixture transmission lines or device under test (D.U.T.) are connected to the network analyzer by means of two 50 ohm coax cables connected to the S-parameter test set which interfaces to the network analyzer. The S-parameter test set has two RF/Microwave ports which can each double as either an output transmitter or input receiver to make the necessary swept S-parameter measurements on the D.U.T. Also one end of the D.U.T can be left open circuited and reflection measurements (S11) in both the frequency and time domain can be made and used to emulate TDR.

In these preliminary experiments the S-parameters have been the dependent variables with the independent variables being frequency, volumetric water content and electrical conductivity. These experiments are being conducted on representative sand soil samples using both the invasive and non-invasive types of transmission lines. The test ranges of these independent variables are listed in Table 2:

Table 2
Test ranges of the independent variables for the preliminary experiments

Frequency:	45 MHz to 32 GHz
Water Content:	0 to 0.33 (~saturation)
Electrical Conductivity:	0 to 11 dS/meter (Soil-Water mix)

In the proposed Ph.D. portion of this research the S-parameters will be measured under the following comprehensive set of conditions (Table 3) for both the invasive as well as the two different non-invasive transmission line patterns mounted on both the top and bottom of the fixtures. The results of these tests will be used to validate the models and dictate any further necessary refinements to the models. Once optimized, the models will be inverted to develop an algorithm to determine water content θ and electrical conductivity σ from an FFT performed on a TDR trace. Accuracy and measurement uncertainty of determining θ and σ will then be quantified.

Table 3
Test conditions for the comprehensive model validations

Non-Saline Conditions:

Open Air (no soil or water)   Moderately Wet Soil (θ = 0.15)
Dry Soil (θ = 0)   Moderately Wet Soil (θ = 0.20)
Nearly Dry Soil (θ = 0.02)   Very Wet Soil (θ = 0.25)
Slightly Wet Soil (θ = 0.05)   Saturated Soil (θ = 0.33).
Slightly Wet Soil (θ = 0.10)

Saline Conditions (approximate values):

Saturated Soil (σ = 0 dS/m, θ = .33)   Saturated Soil (σ = 0.33 dS/m, θ = .33)
Saturated Soil (σ = 0.011 dS/m, θ = .33)   Saturated Soil (σ = 1.1 dS/m, θ = .33)
Saturated Soil (σ = 0.033 dS/m, θ = .33)   Saturated Soil (σ = 3.3 dS/m, θ = .33)
Saturated Soil (σ = .11 dS/m, θ = .33)   Saturated Soil (σ = 11 dS/m, θ = .33).

Very Wet Soil (σ = 10 dS/m, θ = .25)   Slightly Wet Soil (σ = .2 dS/m, θ = .05)
Moderately Wet Soil (σ = 5 dS/m, θ = .20)   Nearly Dry Soil (σ = .1 dS/m, θ = .02)
Moderately Wet Soil (σ = 1 dS/m, θ = .15)   Very Dry Soil (σ = 0 dS/m, θ = 0)
Slightly Wet Soil (σ = .3 dS/m, θ = .10)   Open Air (no soil or water)

In the preliminary experiments water content was varied by initially filling the fixtures to saturation and then allowing a portion of the water to evaporate off of the top to drop the water content to lower levels. The fixtures were weighed frequently (gravitational constant calibrated out to give mass) and equation 1 was used to determine when the proper water content was obtained (the dry mass was determined before the start of the initial experiments). After the desired water content was obtained the fixtures were sealed and allowed to reach equilibrium for 24 hours before measurements were taken. Although this last step was performed to improve the homogeneity of the water in the fixture there was evidence (see results section) of some localized drying and air gaps near the fixture top due to this drying method. There was also some evidence of excess water or water films near the fixture bottom. In the proposed ongoing research, attempts

will be made to improve or lessen these problems or at least account for them in some way.

The different bulk electrical conductivities were obtained in the preliminary experiments by adding progressively more saline water to the fixtures after letting a portion of water evaporate off of the fixture from the previous measurement. The water content was brought back to saturation for each measurement when the more saline water was added. Electrical conductivity was measured on the water solutions that were added to the fixture. The conductivities for the medium under test (saturated cases) were estimated from that predicted by the mixing of the solutions of known conductivity. Direct measurement of the bulk conductivity of the soil-water mix in the fixtures during the preliminary validations was initially attempted by measuring the dc resistance across the transmission lines in the fixture but these measurements were not accurate due possibly to air gaps and other limitations which created measurement errors. It was further concluded that measuring the conductivity directly on the fixtures could actually change the conductivity due to galvanic type reactions caused by passing a direct current through the medium (required to measure resistance). The following equation was used together with external solution conductivity measurements to estimate solution conductivity in the fixture:

$$10 * (EC_w) = Meq \: / \: Liter \: of \: Solute \: in \: Solution \: Mix.$$

Where

EC_w = Electrical Conductivity of the Solution in dS/M
Meq / Liter = milli-equivalents / liter
= milli-Molar for single valence salt solutions (e.g. NaCl solution).

The solute concentration in the fixture water was estimated at each measurement level by knowing the history of what water samples were added along with their respective solute concentrations. The conductivity of the soil-water mix was then approximated as follows:

$$EC = Conductivity \: of \: Soil\text{-}Water \: mix \cong ((Meq/l \: of \: solute \: in \: fixture \: water) \: / \: 10)*(\theta^2)$$

Once the highest conductivity was achieved (~11 dS/m) then water was allowed to evaporate off and measurements were made at lower water contents with conductivities estimated in a similar fashion (with the assumption that all the solute was preserved in the fixture and all stayed in solution (i.e. no precipitation)).

In the proposed ongoing research, improved methods will be investigated to further control the electrical conductivity in the fixture and raise the confidence level on what the bulk conductivity actually is for the soil-water mix. Methods to measure the bulk conductivity directly in the fixture without changing the conductivity (due to galvanic reactions) will also be investigated in the ongoing research. One such method might be to measure the conductivity using an AC current (10 Hz < f < 100 kHz) instead of a DC current so as to reduce net corrosive or electrolytic reactions at each electrode. The current would be sent between the conductors of the invasive parallel wire transmission line and the resulting AC voltage measured across the conductors (at the same end or connector where the current enters and leaves the probe). The voltage and current waveforms could be measured and analyzed by an oscilloscope or other analog sensing circuit (that includes an analog / digital converter) and using the current as a reference, the voltage waveform could be divided into an in-phase (real term) and quadrature (imaginary term or component of waveform that is 90 degrees out of phase). The in-phase voltage component divided by the current would give resistance from which conductivity could be obtained. The quadrature term of the voltage could be used to determine the low frequency capacitance between the lines which could be another way to estimate dielectric constant. At very low frequencies the quadrature term might be small enough to be ignored which would allow simple 4-connection AC multimeter measurements for determining conductivity. These methods will be investigated in the research to follow.

In both the preliminary tests as well as in the proposed ongoing research: two of the test fixtures are being used for the saline condition tests and the other two fixtures are being used for the non-saline condition tests. For both the saline and non-saline conditions,

one fixture has the 3 conductor non-invasive coplanar microstrip circuit board transmission line pattern on top and bottom of the fixture and the other fixture has the 2 conductor balanced microstrip non-invasive circuit board transmission line pattern on top and bottom of the fixture. In all cases S11 and S21 (both magnitude and phase) are measured with both ends of the transmission lines connected to a 50 ohm coaxial cable as well as S11 measured (both magnitude and phase) with the opposite end of the transmission line terminated in an open circuit. All of these measurements are frequency domain measurements. Time domain data is also collected off the network analyzer, using its built in IFFT capability, for the case of S11 with the opposite end of the transmission line open circuited. Because of the symmetry of the test fixtures, S12 and S22 yield similar results to S21 and S11 (assuming all cables and connectors are OK) and so only S21 and S11 results have been and will be used.

The comprehensive validations will result in 216 sets of data for the non-saline conditions and 384 sets of data for the saline conditions giving a total of 600 sets of data. These comprehensive results will be summarized and discussed in the Ph.D. dissertation. Each of these data sets contains 401 data points in either the frequency domain (over two different spans: 45 MHz to 32 GHz or 45 MHz to 18.045 GHz) or the time domain (over a 22.2 ns span). Each of these data sets will be processed in Lotus 123 and MathCAD and compared to predictions from mathematical models. The special range of 45 MHz to 18.045 GHz will be used with S11 so that an Inverse Fast Fourier Transform (IFFT) algorithm can be used to generate a time domain picture equivalent to a TDR trace. This IFFT is also a built in feature of the HP 8510 network analyzer and is one of the methods used to generate the "actual time domain data". Another method will be performing an IFFT on the actual network analyzer frequency domain data (for S11) using a combination of MathCAD and Lotus 123 and comparing those results with those predicted from the mathematical models which are also incorporated into MathCAD and Lotus 123. A preliminary subset of these test conditions and their results and comparisons to predictions are summarized in the results section. The more comprehensive results and model refinements will be left for the Ph.D. thesis.

8. PRELIMINARY RESULTS AND DISCUSSION

Some preliminary data sets have been generated which allow comparison of actual measured data to predicted data for both S11 and S21. More comprehensive model validations and refinements will be conducted as described in section 10. Figures 7 through 15 show measured and predicted frequency domain values for S11 and S21 with a 50 ohm termination, as well as S11 in both the frequency and time domain with an open circuit termination, for both an invasive parallel wire transmission line (figures 7 - 11) and a non-invasive 3-conductor coplanar microstrip transmission line (figures 12 - 15) for different water contents and electrical conductivities. The frequency domain prediction models for S11 and S21 with a 50 ohm termination (figures 7-9, 12, and 13) make use of equations similar to 83 and 84 (with additional terms to model multiple impedance changes in the connector/fixture boundaries). The frequency domain prediction models for S11 with an open circuit termination (figures 10a and 14) were obtained from equation 85 (again with additional terms to model multiple impedance changes in the connector/fixture boundaries). The time domain predictions (figures 10b, 11, and 15) were generated by performing an IFFT on the frequency domain predictions of S11 with an open circuit termination.
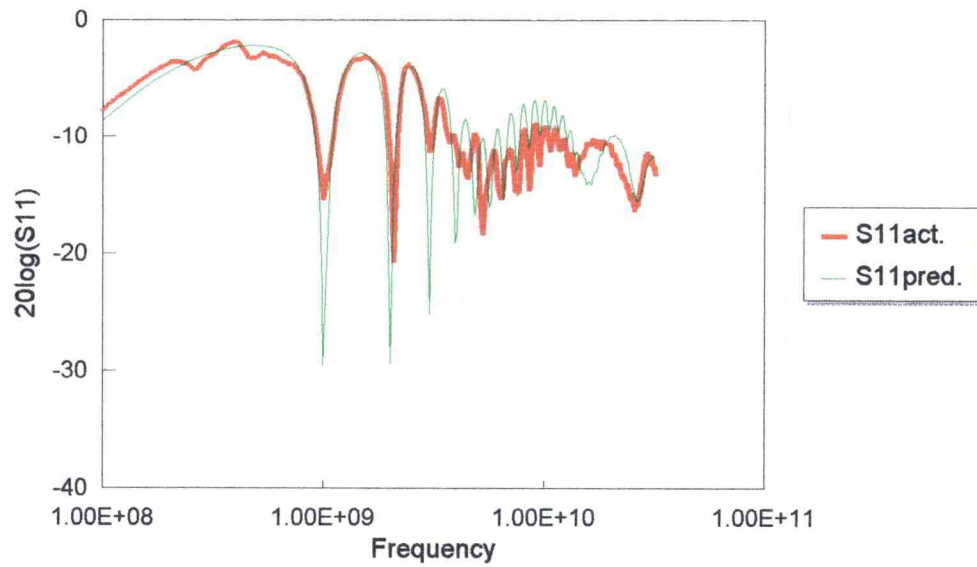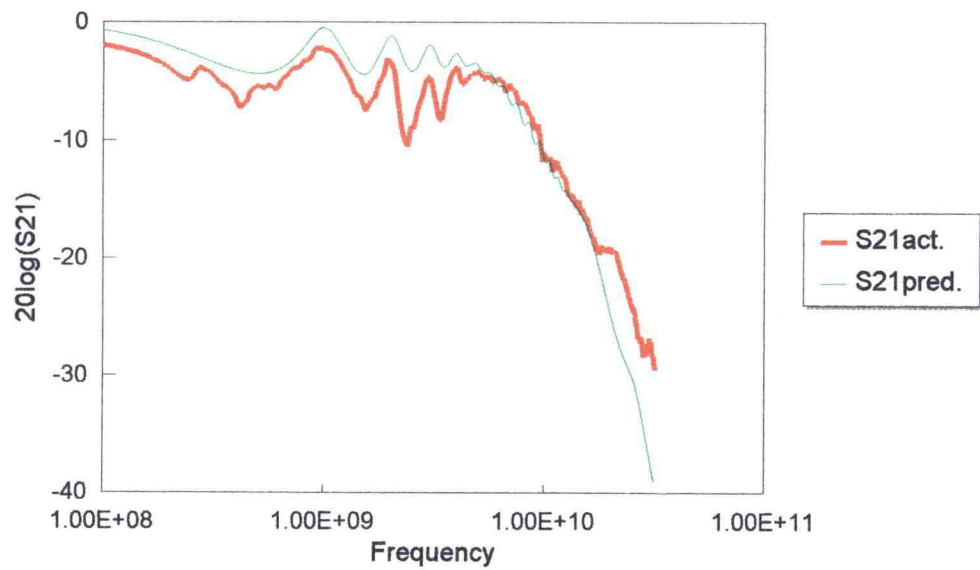
Figure 7. a.) S11 and b.) S21 vs. frequency with actual and predicted data.
Water content = 0.02, EC = 0 dS/m, invasive probe, 50 ohm termination.
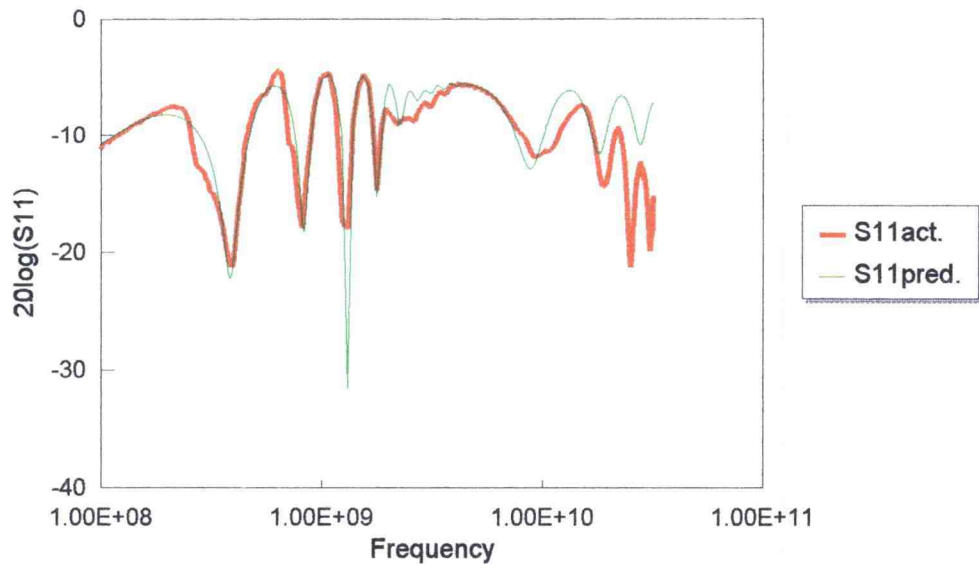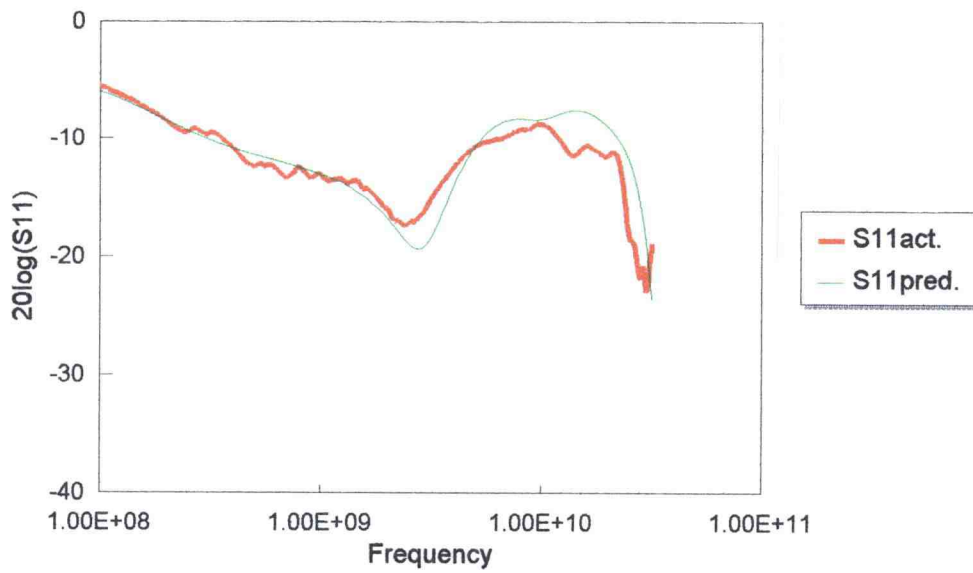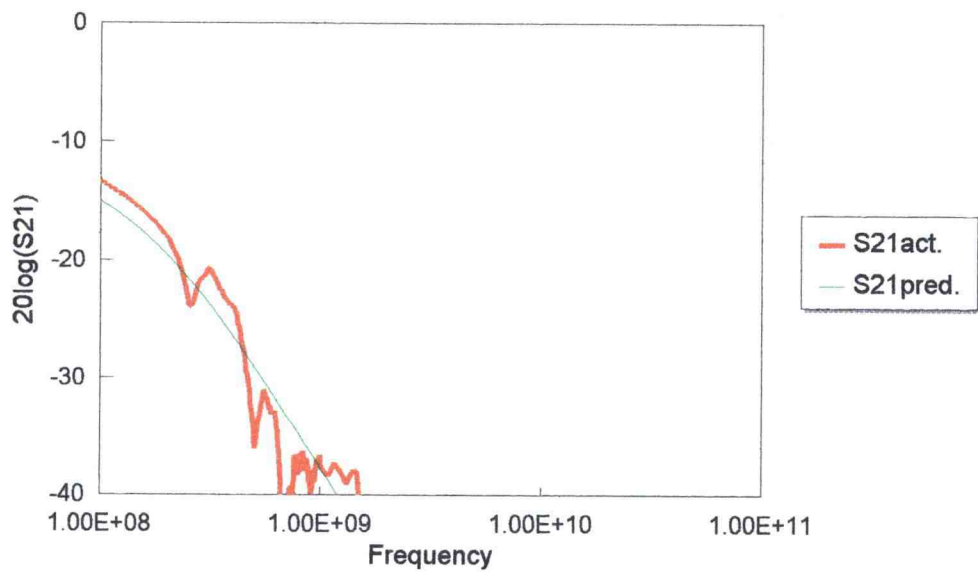
a.)
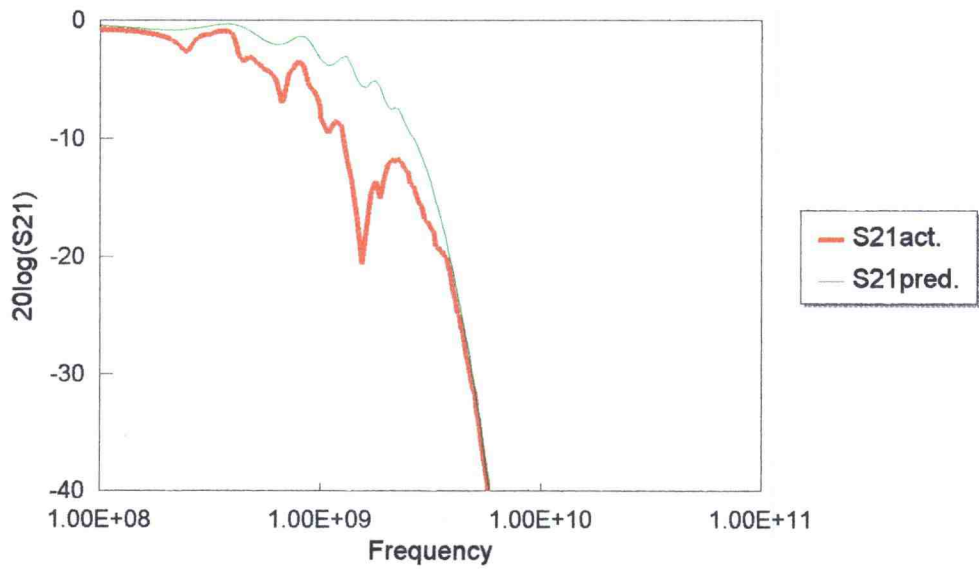
b.)

Figure 8. a.) S11 and b.) S21 vs. frequency with actual and predicted data.
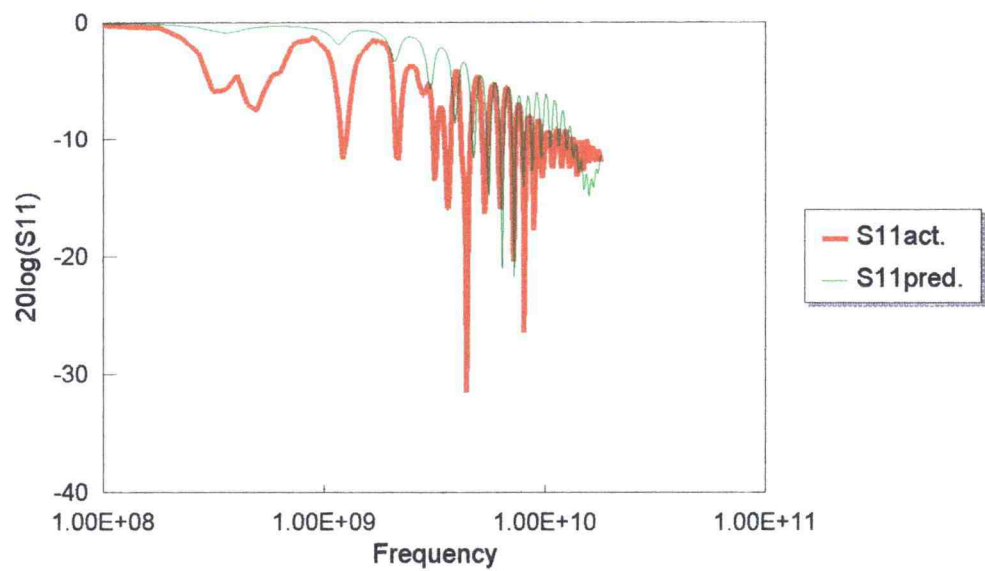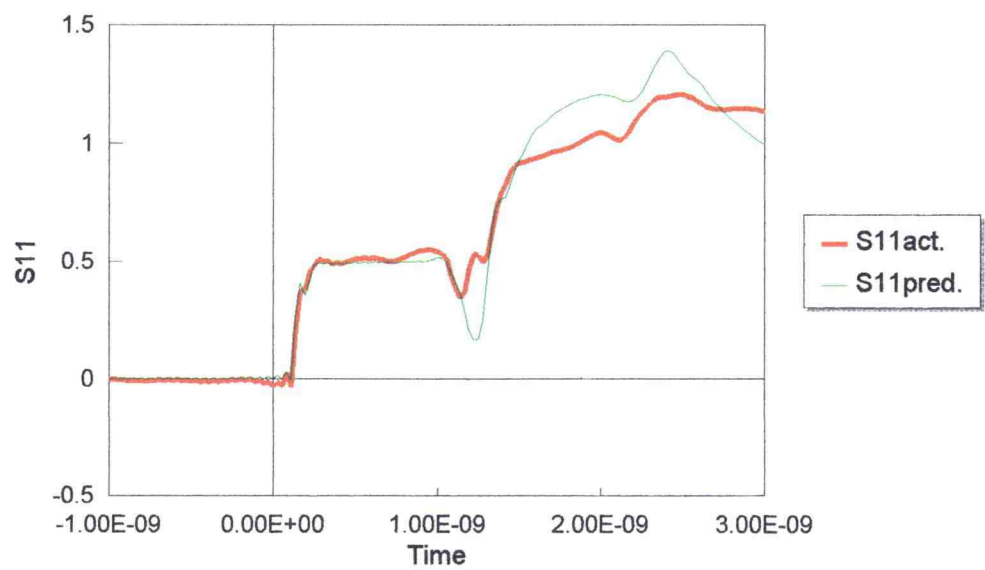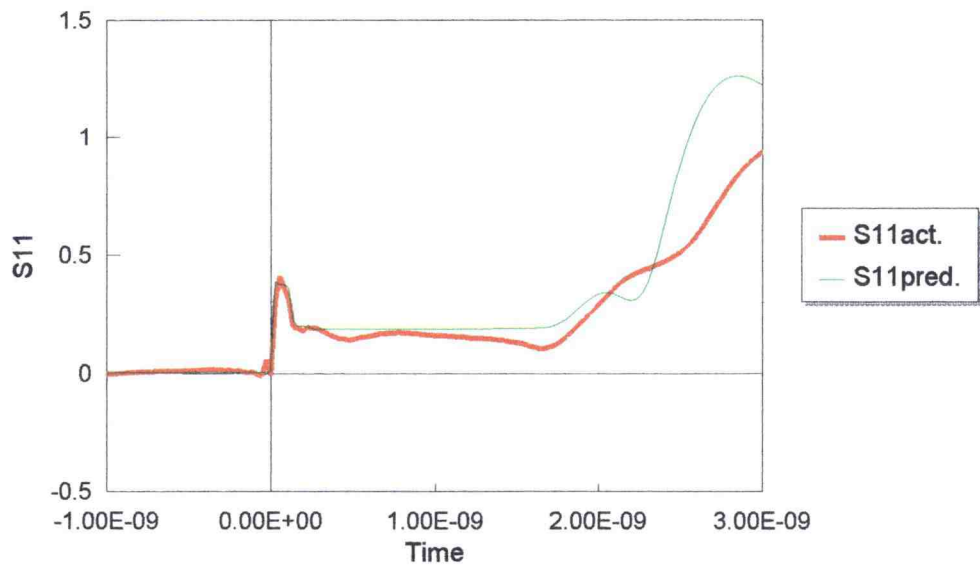Water content = 0.33, EC = 0 dS/m, invasive probe, 50 ohm termination.

Figure 9. a.) S11 and b.) S21 vs. frequency with actual and predicted data.
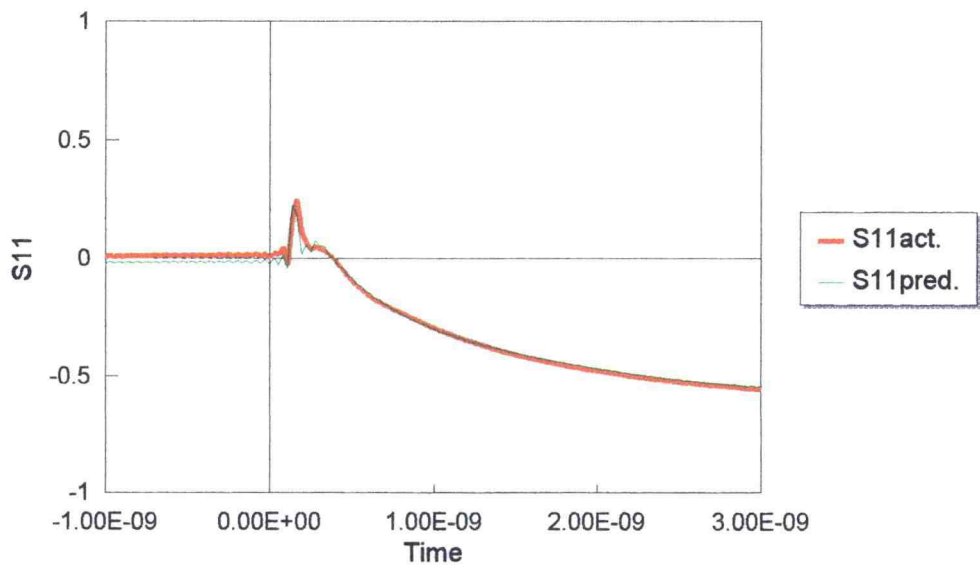Water content = 0.33, EC = 11 dS/m, invasive probe, 50 ohm termination.

a.)

b.)

Figure 10. Actual and predicted data of S11 in the frequency and time domains. Water content = 0.02, EC = 0 dS/m, invasive probe, open termination.
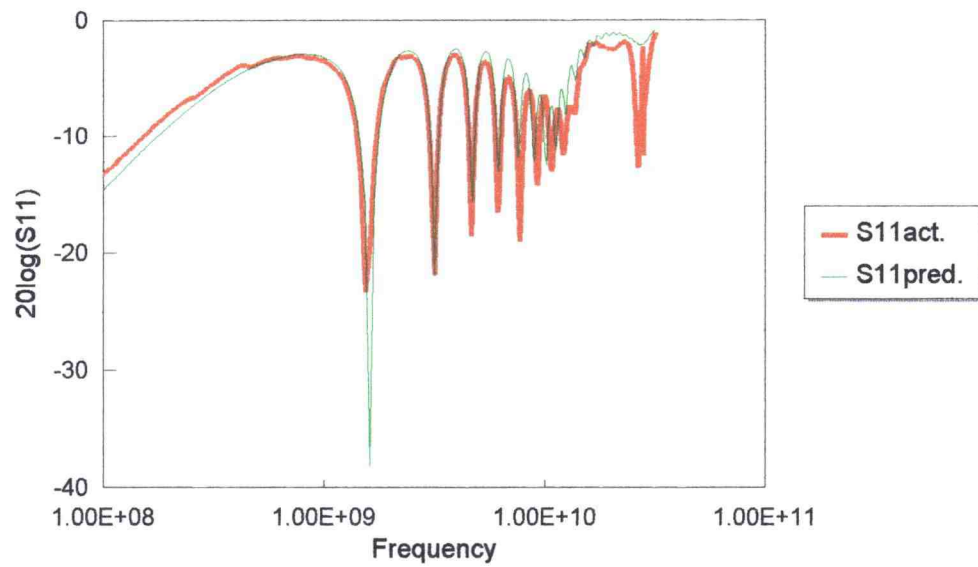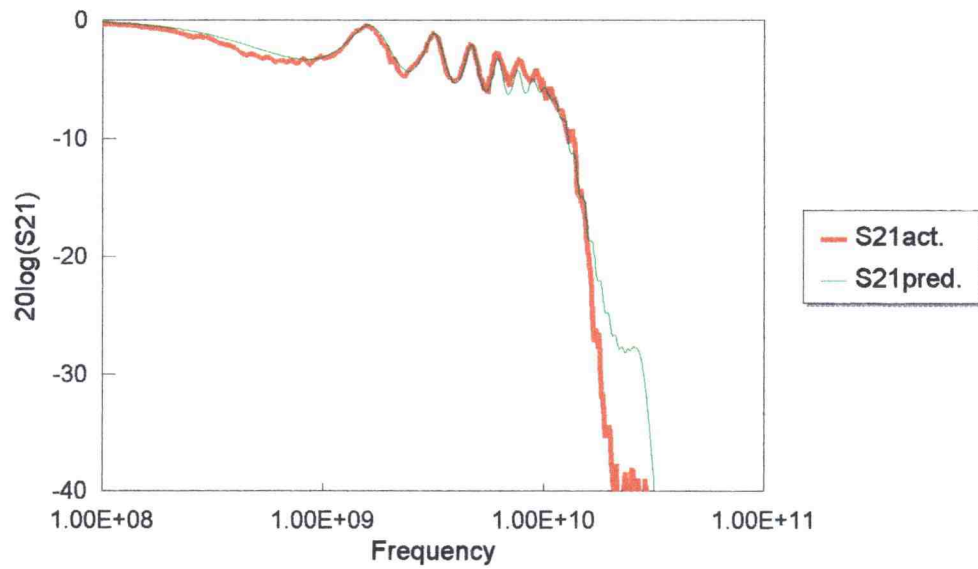
a.)

b.)

Figure 11. Actual and predicted data of S11 in the time domain for a.) EC = 0 dS/m and b.) EC = 11 dS/m. Water content = 0.33, invasive probe, open termination.
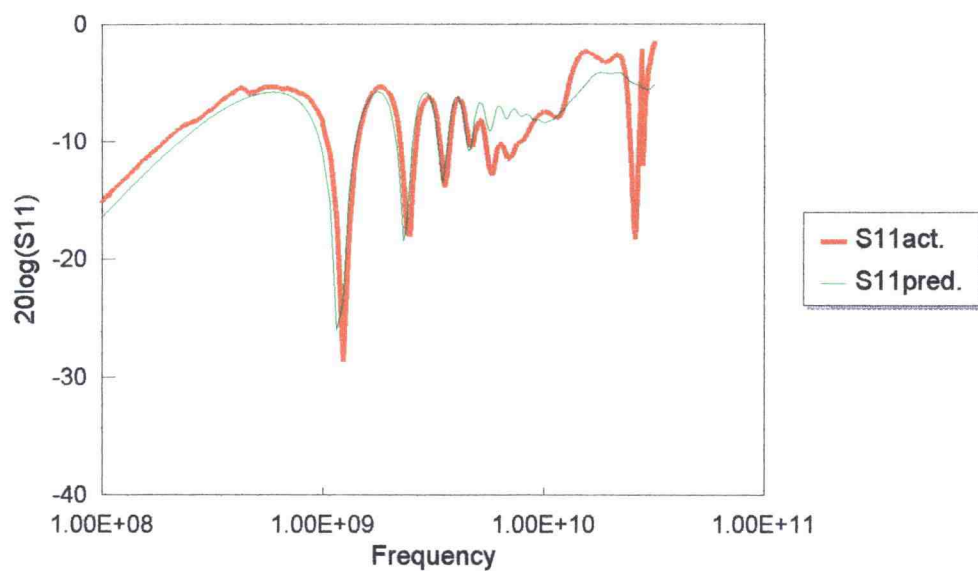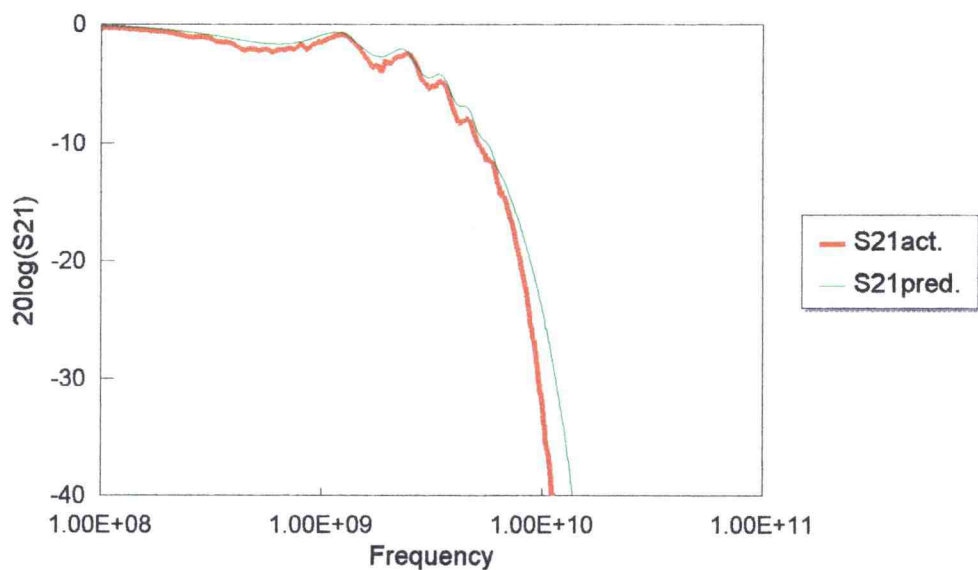
Figure 12. a.) S11 and b.) S21 vs. frequency with actual and predicted data.
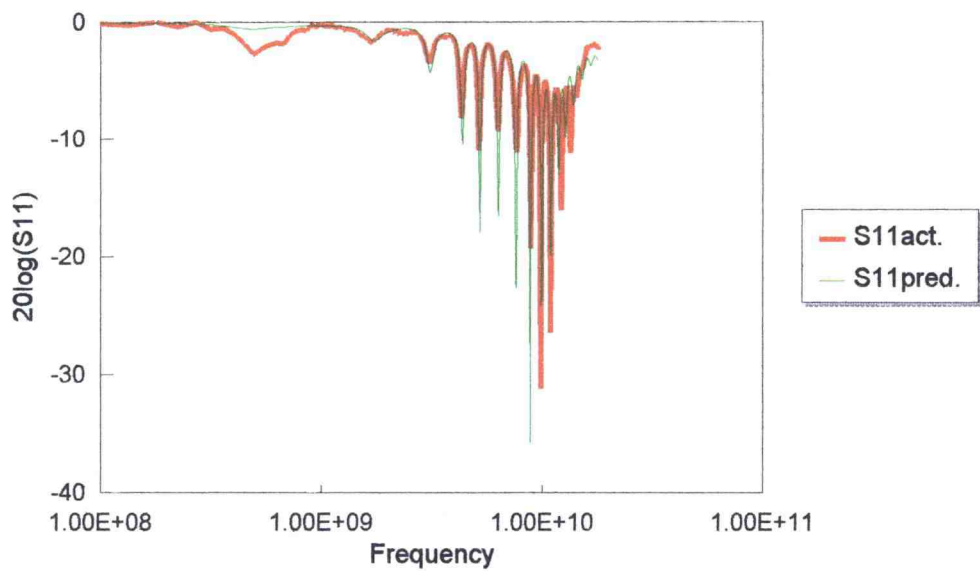Water content = 0.02, EC = 0 dS/m, non-invasive probe, 50 ohm term.

a.)

b.)

Figure 13. a.) S11 and b.) S21 vs. frequency with actual and predicted data.
Water content = 0.15, EC = 0 dS/m, non-invasive probe, 50 ohm term.

a.)
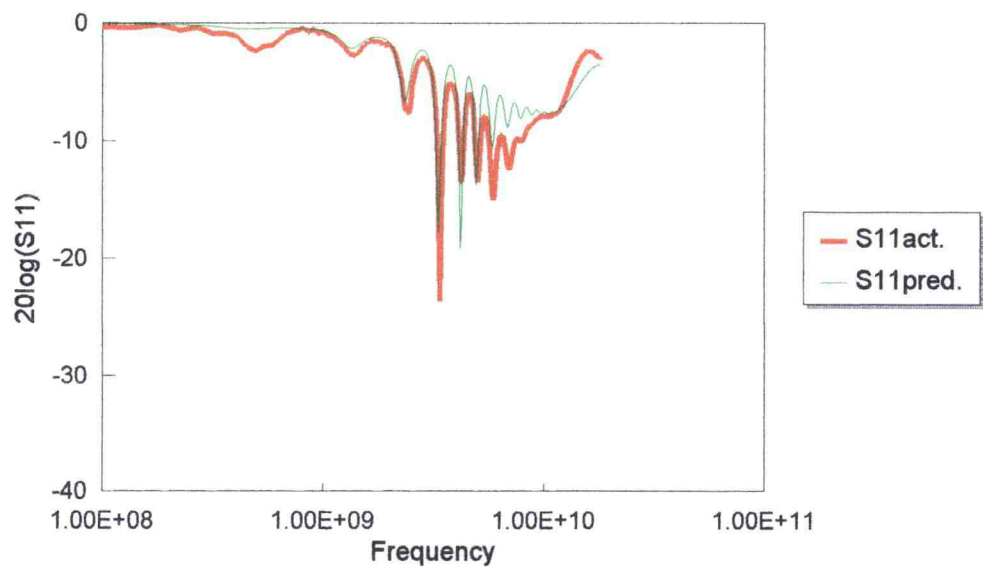
b.)

Figure 14. Actual and predicted data of S11 vs. frequency for a.) water content = 0.02
and b.) water content = 0.15. EC = 0 dS/m, non-invasive probe, open term.

a.)

b.)

Figure 15. Actual and predicted data of S11 vs. time for a.) water content = 0.02
and b.) water content = 0.15, EC = 0 dS/m, non-invasive probe, open term.

8.1 Overall Summary of Results

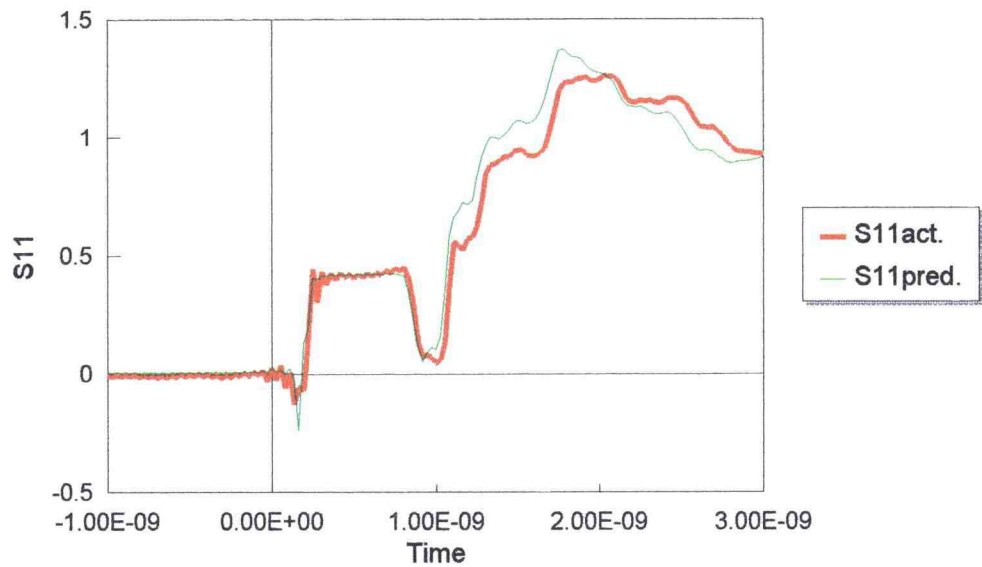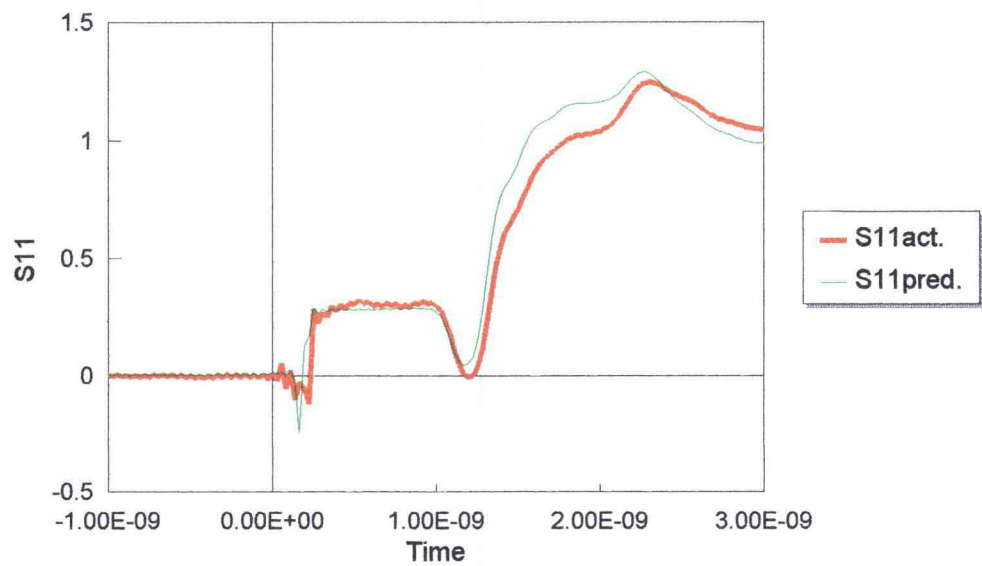The data shows that the models are good predictors of frequency domain performance up to as high as 20 GHz. They also appear to be good predictors of the change of performance with water content and electrical conductivity although many more data points need to be processed to fully validate the models over wide ranges of those parameters. Some of the potential problems that are showing up in these early results are how to properly model non-ideal connectors and boundaries. Non-ideal boundary modeling was especially difficult with the invasive probe where there was a boundary between an unbalanced coaxial cable and a balanced two-wire transmission line. The models will be refined in the ongoing research to account for this. Other problems that were discovered in these preliminary tests were with the non-invasive probe at the fixture top at medium water contents (air gap caused under prediction of phase velocity and therefore over prediction of TDR transit time) and the fixture bottom at saturation (water film caused over prediction of phase velocity and therefore under prediction of TDR transit time and conductivity effects). These air gaps and water films are not problems with the models but instead are problems with the way the fixtures are designed and the way water content is allowed to change in them (evaporating out the top). Methods of reducing these effects or accounting for them will be investigated during the ongoing research. The non-invasive probe at the fixture bottom responded well to water contents in the low to medium range (0 to 0.15 water contents) where no water films were created. These results are shown in figures 12 to 15. Above 20 GHz the assumptions behind the models begin to breakdown such as Transverse-Electric-Magnetic (TEM) wave propagation due to transmission line spacing and connector diameters becoming significant with a wavelength of the traveling wave.

8.2 Invasive Probe Results

The invasive probe results showed good agreement with the prediction models in both the frequency domain and time domain with the exception of slight frequency domain distortion in the lower frequency ranges or at frequencies where the reflected signal from the far end of the transmission line hadn't been greatly attenuated. This slight distortion gave the appearance of some extra loss in S21 or in the transmitted signal as well as some extra ripples or "bumps" in the frequency response of S11 (figures 7 and 8). In the time domain this error appeared to show up in distortion beyond the second reflection (regions less critical to TDR water content measurement). This distortion and extra attenuation did appear to cause errors, however, in modeling the connector and boundary effects at the far end of the transmission line. A slight error in the attenuation and reflection characteristics of the traveling pulse is compounded in time (to the right) especially beyond the second reflection. A likely source of these slight errors is due to non-ideal reflection and loss mechanisms at the boundary between the unbalanced driving coaxial cable and the balanced two wire transmission line. This effect will be investigated and the models refined to account for it in the ongoing research. On the whole the preliminary results show good agreement with the prediction models for the water contents and conductivities shown.

8.3 Non-Invasive Probes Results

The non-invasive probe models are more complex than the invasive probe models. The mixing model becomes more complex since a fourth component (circuit board dielectric (RT-Duroid)) has to be included in the model. Equations 63, 64 and 66 have to be modified to what is shown in equations 94 - 96 for the non-invasive probes:

Non-Invasive Propagation Constant:

$$\gamma_{TCB} = \sqrt{0.5\left[(\gamma_s(1-\phi) + \gamma_W(\theta) + \gamma_A(\phi - \theta))^2 + (\gamma_{CB})^2\right]} = \alpha_{TCB} + j\beta_{TCB} \qquad (94)$$

Effective Non-Invasive Phase Velocity:

$$V_{pTCB} = \frac{\omega}{\beta_{TCB}} \qquad (95)$$

Effective Non-Invasive Dielectric Constant:

$$\varepsilon_{eff\,CB} = \left(\frac{1}{V_{pTCB}\sqrt{\mu_r\mu_0\varepsilon_0}}\right)^2 \qquad (96)$$

Equation 94 assumes that the soil and the circuit board are effectively in parallel whereas the individual solid, water and air components of the soil are in series with each other but in parallel with the circuit board material of the non-invasive probe.

The characteristic impedance for the two different types of non-invasive probes are developed in equations 97 - 99:

Non-Invasive Intrinsic Impedance:

$$\eta_{TCB} = \frac{j\omega\mu}{\gamma_{TCB}} \tag{97}$$

Non-Invasive (3-conductor) Coplanar Microstrip Impedance (Ramo et al., 1994):

$$Z_{TCB} = \left(\frac{1}{\pi}\right)\left[\ln\left(2\sqrt{\frac{a}{w}}\right)\right]\eta_{TCB} \tag{98}$$

Non-Invasive (2-conductor) Balanced Microstrip Impedance:

$$Z_{TCB} = \left(\frac{1}{\pi}\right)\left[\cosh^{-1}\left(\frac{b}{w}\right)\right]\eta_{TCB} \tag{99}$$

where a   =   spacing between outer two traces on 3-trace non-invasive probe.

b   =   spacing between two traces on 2-trace non-invasive probe.

w   =   width of center microstrip trace on 3-trace non-invasive probe
or width of each trace on 2-trace non-invasive probe.

γ_s =   Propagation Constant in solid phase (fused quartz in our soil).

γ_w =   Propagation Constant in water or liquid phase.

γ_A =   Propagation Constant in Air.

γ_{CB} =   Propagation Constant in Circuit Board (RT-Duroid)

γ_{TCB} =   Overall Propagation Constant of Overall Circuit Board-Soil Mix

η_{TCB} =   Intrinsic Impedance of overall circuit board-soil mix.

Z_{TCB} =   Characteristic Impedance of microstrip transmission line.

ε_{effCB} =   Effective relative permittivity or dielectric constant.

and all the other parameters are as defined earlier.

Some problems were encountered with the non-invasive probes employed in these preliminary validation experiments. In the case of the circuit board at the fixture top, air gaps at the circuit board-soil boundary created delayed responses to water content until saturation was achieved. The circuit board at the bottom responded much better than that at the top, in better agreement to predictions, but still has some problems at saturation due probably to a water film leading to a localized higher dielectric constant and thus slowing of the wave propagation. These are problems that will be addressed in the ongoing research.

Figures 12 - 15 show that there is very good agreement between the non-invasive model predictions and actual results when water films and/or air gaps are not present. The results shown are for the 3 conductor coplanar transmission line. These results also show that non-ideal connectors and boundary interfaces can be modeled fairly accurately when the probe is also an unbalanced transmission line as opposed to the balanced invasive two wire lines.

9. CONCLUSIONS

Several soil moisture measurement techniques were reviewed with the conclusion being that electromagnetic techniques, such as Time Domain Reflectometry, probably offer the greatest promise in balancing all of the issues of measurement accuracy, resolution, reasonable imaging volume, measurement speed, response time to changing soil conditions, potential for reduced soil disturbance, reduced calibration, and ability to measure both water content and electrical conductivity. Therefore a model based on the theory of electromagnetics and S-parameter network theory was developed to enhance the usefulness of TDR as a soil water content and electrical conductivity measurement tool over wide ranges of those parameters.

Preliminary validation tests have shown that the mathematical models for electromagnetic wave propagation appear to be good predictors for S11 and S21 for frequencies up to 20 GHz for both the invasive and bottom fixture non-invasive probes when localized air gaps or water films are not present. Above 20 GHz some of the underlying assumptions of the models breakdown such as TEM wave propagation due to connector diameters and transmission line conductor spacings becoming significant with a wavelength. Fortunately, the important TDR spectrum lies below 20 GHz.

One of the problems uncovered in these early results with the invasive probe was the difficulty of modeling non-ideal connectors and boundaries when there was a boundary between unbalanced coax cables and balanced parallel wire transmission lines. Extra loss occurs in the critical TDR spectrum due to this effect and this will be dealt with in model refinements in the research to follow.

The predictions agreed very well with actual data for the non-invasive probe in regions where air gaps and/or water films were not present (low to medium water contents on the fixture bottom). However, problems with air gaps (intermediate water contents

with fixture top probes) and water films (high water contents with fixture bottom probes) are a real issue for these types of probes and will have to be dealt with in the ongoing research. The response of the non-invasive probes will be less than the invasive probes even under good conditions due to the presence of a solid dielectric material over one-half of the volume of influence of the electromagnetic waves. The preliminary results do show that there is good promise for non-invasive TDR probes if these air gaps and water films are accounted for or eliminated.

It appears that electrical conductivity can be accurately determined from the models by measuring the slope or rolloff of the time domain waveforms for conductivities above 1 dS/m and can be determined at all levels of conductivity by looking at the frequency domain data for S21 (amount of intermediate frequency rolloff (100 MHz to 5 GHz)). More research needs to be conducted in this area. The models are good predictors of conductivity effects for the invasive probes and probably would be applicable as predictors of conductivity effects in the non-invasive probes if air gaps and water films were better accounted for or modeled near the probe surfaces.

The models and data show that dispersion and attenuation distort the second TDR reflection when electrical conductivity is high. The characteristic impedance also drops off with lower frequencies when the electrical conductivity is high giving a "high pass" filter step response in the time domain.

Finally, high frequency rolloff or attenuation and dispersion (above 1 GHz) are seen to occur even in the absence of dc electrical conductivity due to the efficient consumption of energy near and around the self resonant frequency of the polar water molecules. This can be modeled accurately with the Cole-Cole model for the imaginary and real portions of the dielectric constant.

10. PROPOSAL FOR ONGOING RESEARCH

10.1 Statement of Problem

Water conservation and water quality improvement have, in recent decades, become issues of importance in all areas of the world. The ability to accurately measure soil water content and electrical conductivity or salinity, over a wide variety of conditions, has therefore also risen in importance.

Time Domain Reflectometry (TDR) has become a popular method, over the last decade, of measuring volumetric soil water content, due to the fact that fast measurements can be taken with a minimum amount of soil disturbance and without the use of radioactive methods. Irrigated agriculture is one area where accurate soil water content measurements can be of value. One of the typical problems encountered in irrigated agriculture (especially in semi-arid and arid climates such as the Imperial Valley of California) is the problem of salinity in the soil after irrigating for several years. Salts from the irrigation water are deposited in the soil and build up over years due to insufficient winter rains or lack of sufficient high quality irrigation water to leach the salts. Therefore, accurate methods of measuring soil water content in the presence of electrical conductivity or salinity would be of great value. Also, the ability to accurately measure the conductivity itself, would be of great value in terms of assessing water quality. Finally, methods that make these measurements with a minimum amount of soil disturbance, or even non-invasively, would increase utility.

TDR, and other soil moisture measurement technologies such as capacitive probes and ground penetrating radar (GPR), rely on changing electromagnetic properties of the soil when water is present. They rely on the fact that as moisture content goes up, the electrical permittivity (and therefore, the dielectric constant) of the soil mix also goes up which is a good assumption in the absence of electrical conductivity (or salinity).

In the presence of electrical conductivity or salinity, however, moisture measurement techniques which rely on dielectric constant and phase velocity changes, encounter three problems: First, the higher the frequency, the more the wave is attenuated in the medium and therefore the less distance it can penetrate into the medium. Second, different frequencies travel at different velocities which will lead to dispersion of a waveform with multiple frequency components (i.e., TDR step waveform). Finally, the impedance of a transmission line, inserted into a saline medium, drops off with lower frequencies, which gives frequency-dependent reflection characteristics at the interface of the medium. All of these problems will lead to errors in the measurement of water content with TDR and other electromagnetic methods in the presence of high salinity or electrical conductivity.

Another problem with the present approach to TDR water content measurement methods is the degree to which empirical regression equations are relied upon to determine water content from the medium dielectric constant, and/or directly from the velocity (phase velocity) of the traveling wave. This dependence on regression equations usually means that a TDR system must be calibrated over several water contents for each different type of soil it is being used on. This limits the flexibility of TDR as a field instrument that can be taken from location to location and quickly and easily measure water content. Lengthy calibrations need to be run first on any new field or soil type that is to be measured. Therefore, there is also a need for an algorithm that requires a minimum amount of calibration to use TDR, on new soil types or at different field locations, so as to make TDR a very flexible instrument that can easily be set up at new field locations.

10.2 Statement of Opportunity or Question

The question this research project attempts to answer is the following: Can an analytically derived mathematical model based on the first principles of electromagnetic theory, S-parameter modeling and FFT and IFFT algorithms, be used in a software algorithm to make a field compatible TDR water content and electrical conductivity (or salinity) measurement system that is accurate over wide ranges of those parameters?

This research project will make use of the ability to accurately model TDR wave propagation over wide ranges of water content and electrical conductivity, in the development of a commercial algorithm (software product) to be used by TDR systems to accurately measure water content, even when the conductivity is high, as well as measure conductivity itself. This approach is fundamentally different from that now used in the industry, where no quantitative models of wave propagation have been used. The improved models in this algorithm will also greatly reduce the amount of calibration necessary, when a TDR system is installed into a new site, due to improved mixing models of the three phases of liquid, gas and solids and how they effect the electromagnetic properties. Calibration would only be required at a maximum of two water contents and possibly only one water content.

These improved models are based on the merging of the two sciences of electromagnetics and soil physics using the well-established existing models from each field together in a way that hasn't been attempted to any significant degree to this point by other research efforts. Accurate TDR predictions over large ranges of conductivity and water content are possible with these models which can be reversed and turned into algorithms to determine conductivity and water content from the measured waveforms. It is this second form of algorithm which will be developed, validated, and tested in this research project.

This product could have many commercial applications. Since all current TDR systems store the entire TDR waveform trace, this new software product could be adopted by all current TDR users (i.e. retrofitted into their systems). A software product of this type could easily be extended beyond just TDR systems. The development of much lower cost water content and electrical conductivity measurement systems, using these algorithms, could be envisioned using other electromagnetic methods. The focus in this research effort will be on TDR systems, however, with extensions to other technologies being the subject of future research and development efforts.

10.3 Technical Objectives

The objectives for this research project are listed as follows:

- MODEL VALIDATIONS: To complete the preliminary model validations and refinements by comparing the predictions to actual results obtained by network analysis and performing iterations on the models for both invasive and non-invasive probes.

- CONTROL TESTS: To measure and compile TDR traces (or waveforms) over a wide range of soil water contents and electrical conductivities (or salinities) with different soil types using both standard probes and non-invasive probes. Also independently measure water content and conductivity using gravimetric analysis and conductivity meters respectively.

- ALGORITHM DEVELOPMENT: To refine and incorporate the recently developed mathematical models into an algorithm which takes measured TDR waveforms and performs an FFT to give S11 vs. frequency. From that result the parameters of soil dielectric constant, water content and electrical conductivity can be extracted.

- DETERMINATION OF FEASIBILITY: To conclude on the feasibility of using these models, as a commercial software product, with existing TDR measurement systems to be able to accurately measure water content and electrical conductivity over a wide range of soil conditions with a minimum amount of calibration. Also conclude on the feasibility of non-invasive TDR probes.

- Ph.D. THESIS: To report all the test results and provide a written answer to the stated question of this research. If the answer to the question shows the algorithm to be feasible then the Ph.D. thesis will also contain a chapter proposing the next phase of research and development. The thesis will also contain chapters showing all the background theory of the algorithm.

10.4 Research Plan

The key objective of this phase of research is to determine the feasibility of "inverting" the developed electromagnetic model for wave propagation to interpret TDR signals. The goal is to fit an observed TDR trace to the model parameters of soil dielectric, water content and electrical conductivity. This would effectively take TDR measurements from an empirical calibration equation approach to an analytical model, potentially yielding much higher precision and tolerable range in measurement of all parameters over a wide range of soil types, soil water contents and soil electrical conductivities. The steps of the test or research plan are given as follows:

1.) Complete the model validations and refinements as spelled out in the materials and methods section of this thesis using the test results from the HP8510B network analyzer.

2.) Obtain data set from 1502b TDR system (most widely used in the field) for the following range of soil conditions using standard probes as well as non-invasive probes:

electrical conductivity	volumetric water content	soil types
0 to 20 dS/m	0 to 0.5 (or saturation)	sand, silt and clay

3.) Perform an FFT (Fast Fourier Transform) on the time domain data to obtain plots of S11 vs. frequency over the range of 100 MHz to 10 GHz.

4.) Generate an algorithm which fits the prediction model to the actual data by varying the parameters of water content and electrical conductivity and using known values for the dielectric constant vs. frequency for water as well as assumed values of dielectric constant for the dominant solids in the soil (e.g. quartz for sandy soils). Use numerical and iterative methods to minimize the sum of squares error between the model and the actual data.

The results will be compiled and plotted, showing both the actual data and the fitted model curves. The models will be assessed and improved where necessary, using nonlinear regression and/or numerical methods and possibly additional cascaded stages in the S-parameter models if needed. The improved models will be further validated against existing test data to determine their feasibility for use in a commercial TDR product to get accurate field measurements, of water content and electrical conductivity, over a wide range of conditions. The models will also help in the selection of optimum frequencies or frequency ranges and pulse shapes to maximize accuracy and resolution of the measurement as well as reduce the cost.

10.5 Potential Commercial Applications

1.) Field TDR measurement system that accurately measures water content and electrical conductivity over a wide range of conditions with a minimum amount of calibration.

2.) New types of TDR probes that improve contact to the soil or increase the zone of influence to lessen the effects of air gaps (low to medium water contents) and water films (high water contents). The greatest application would be with non-invasive probes.

3.) Software algorithms that could improve the accuracy of other non-agriculture applications of TDR as well as other instrumentation that rely on accurate modeling of electromagnetic wave propagation through medium that contain saline water or other liquids. Organic materials could be identified due to their self resonant frequencies.

4.) Improved non-invasive TDR or other types of electromagnetic instruments that could measure the water content and electrical conductivity of several different types of media such as soil, concrete, wood, food products, and others, with no disturbance to the sample being measured.

BIBLIOGRAPHY

Abraham, R.J., J. Fisher and P. Loftus. 1988. *Introduction to NMR Spectroscopy*. New York: John Wiley & Sons, Inc.

Anderson, R.W. 1967. S-parameter techniques for faster, more accurate network design. *Hewlett-Packard J.* 18:1-12, Palo Alto, CA.

Arcone, S. 1986. Conductivity limitations in single-reflection time-domain reflectometry. *J. Phys. E: Sci. Instrum.* 19:1067-1069.

Avery, T.E., and G.L. Berlin. 1992. *Fundamentals of Remote Sensing and Airphoto Interpretation*. fifth edition. Upper Saddle River, New Jersey: Prentice Hall.

Bailey, A.E. 1989. *Microwave Measurements*. 2nd Addition. Peter Peregrinus Ltd. 28-73.

Bertolini, D., M. Cassettari, G. Salvetti, E. Tombari, and S. Veronesi. 1990. Time domain reflectometry to study the dielectric properties of liquids: some problems and solutions. *Rev. Sci. Instrum.* 61:450-456.

Bristow, K.L., G.S. Campbell, and Kees Calissendorff. 1993. Test of a heat-pulse probe for measuring changes in soil water content. *Soil Sci. Soc. Am. J.* 57:930-934.

Campbell, J.E. 1990. Dielectric properties and influence of conductivity in soils at one to fifty megahertz. *Soil Sci. Soc. Am. J.* 54:332-341.

Cuenca, R.H.. 1989. *Irrigation System Design*. Englewood Cliffs, New Jersey: Prentice Hall.

Cuenca, R.H., J. Brouwer, A. Chanzy, P. Droogers, S. Galle, S.R. Gaze, M. Sicot, H. Stricker, R. Angulo-Jaramillo, S.A. Boyle, J. Bromley, A.G. Chebhouni, J.D. Cooper, A.J. Dixon, J-C. Fies, M. Gandah, J-C. Gaudu, L. Laguerre, J. Lecocq, M. Soet, H.J. Steward, J-P. Vandervaere, and M. Vauclin. 1996. Soil measurements during Hapex-Sahel intensive observation period. In press in: *J. Hydro. Special issue on Hapex-Sahel.*

Dalton, F.N., W.N. Herkelrath, D.S. Rawlins, and J.D. Rhoades. 1984. Time domain reflectometry: simultaneous measurement of soil water content and electrical conductivity with a single probe. *Science (Washington)* 224:989-990.

Dalton, F.N. and M.Th. Van Genuchten. 1986. The time-domain reflectometry method for measuring soil water content and salinity. *Geoderma* 38:237-250.

Dalton, F.N., and J.A. Poss. 1990. Soil water content and salinity assessment for irrigation scheduling using time domain reflectometry: principles and applications. *Acta Hort.* 278, 1:381-393.

Dalton, F.N. 1992. Development of time-domain reflectometry for measuring soil water content and bulk soil electrical conductivity. In *Advances in Measurement of Soil Physical Properties: Bringing Theory into Practice,* ed. G.C. Topp, 143-167. SSSA Spec. Publ. 30. Madison, WI: SSSA.

Dasberg, S. and F.N. Dalton. 1985. Time domain reflectometry field measurements of soil water content and electrical conductivity. *Soil Sci. Soc. Am. J.* 49:293-297.

Eyges, L. 1972. *The Classical Electromagnetic Field.* New York: Dover Publications, Inc.

Flugstad, B.A. 1995. *Characterization of TDR Water Content Measurement Performance in Saline Environments with Invasive and Non-Invasive TDR Probes.* Research Report for Sandia Labs. 110 pages.

Flugstad, B.A., and J.S. Selker. 1996. A model for predicting time domain reflectometry water content measurements in conductive media. In Press: *Water Resour. Res.*

Gadian, D.G. 1982. *Nuclear Magnetic Resonance and its Applications to Living Systems.* Oxford: Clarendon Press.

Gardner, W.H. 1986. Water Content. *Methods of Soil Analysis, Part 1. Physical and Mineralogical Methods.* 9:493-544. Madison, WI: ASA and SSSA.

Halliday D., and R. Resnick. 1977. *Physics.* 3rd edition. New York: John Wiley & Sons, Inc. 334-361.

Harris, R.K. 1986. *Nuclear Magnetic Resonance Spectroscopy.* England: Longman Scientific & Technical.

Heathman, G.C. 1993. Soil moisture determination using a resonant frequency capacitance probe. *1993 summer meeting of Amer. & Can. Soc. of Agric. Eng. paper # 931053.*

Heimovaara, T.J. 1994. Frequency domain analysis of time domain reflectometry waveforms. 1. measurement of the complex dielectric permittivity of soils. *Water Resour. Res.* 30:189-199.

Heimovaara, T.J., W. Bouten, J.M. Verstraten. 1994. Frequency domain analysis of time domain reflectometry waveforms. 2. A four-component complex dielectric mixing model for soils. *Water Resour. Res.* 30:201-209.

Helszajn, J. 1978. *Passive and Active Microwave Circuits.* 1-23. New York: John Wiley & Sons, Inc.

Herkelrath, W.N., S.P. Hamburg, F. Murphy, 1991. Automatic, Real Time Monitoring of Soil Moisture in a Remote Field Area with Time Domain Reflectometry. *Water Resour. Res.* 27:857-864.

Hewlett-Packard. 1972. S-parameter design. *Hewlett Packard Application Note* 154:1-13. Palo Alto, CA.

Hinedi, Z.R., Kabala, Z.J, T.H. Skaggs, D.B. Borchardt, R.W. K. Lee, and A.C. Chang. 1993. Probing soil and aquifer material porosity with nuclear magnetic resonance. *Water Resour. Res.* 29:3861-3866.

Hinedi, Z.R., A.C. Chang, and M.A. Anderson. 1995. NMR relaxation of water saturated porous matrices. quantification of microporosity. In *Vadose Zone Hydrology: Cutting Across Disciplines,* ed. D. Silva, 65-66. University of CA., Davis: Kearney Foundation of Soil Science International Conference Proceedings.

Hogan, B.J. 1986. One-sided NMR sensor system measures soil/concrete moisture. *Design News.* May 5, 1986. 108-111.

Jay, F., and J. A. Goetz. 1984. *IEEE Standard Dictionary of Electrical and Electronics Terms.* New York: IEEE, John Wiley & Sons, Inc.

Jin, Jianming., 1993. *The Finite Element Method in Electromagnetics.* New York: John Wiley & Sons, Inc.

Jury, W.A., W.R. Gardner, and W. H. Gardner. 1991. *Soil Physics.* Fifth Edition. New York: John Wiley & Sons, Inc.

Kelly, S.F., J.S. Selker, and J.L. Green. 1996. Using short soil moisture probes with high-bandwidth time domain reflectometry instruments. *Soil Sci. Soc. Am. J.* 59:97-102.

Klute, A. 1986. *Methods of soil analysis part 1: physical and mineralogical methods second edition.* Madison, WI: ASA and SSSA.

Kraszewski, A.W. and S.O. Nelson. 1992. Wheat moisture content and bulk density determination by microwave parameters measurement. *Can. Agric. Res.* 34:327- 335.

Magnusson, P.C., G.C. Alexander, and V.K. Tripathi. 1992. *Transmission Lines and Wave Propagation*. 3rd edition. Ann Arbor: CRC Press.

Matzkanin, G.A. and R.F. Paetzold. 1982. Measuring soil water content using pulsed nuclear magnetic resonance. In ASAE Winter Meetings. Chicago. Paper no. 82-2619. St. Joseph, MI: ASAE.

Milsom, J. 1989. *Field Geophysics*. New York: Halsted Press, John Wiley & Sons, Inc.

Nadler, A., S. Dasberg, and I. Lapid. 1991. Time domain reflectometry measurements of water content and electrical conductivity of layered soil columns. *Soil Sci. Soc. Am. J.* 55:938-943.

Paetzold, R.F., A.D.L. Santos, and G.A. Matzkanin. 1987. Pulsed nuclear magnetic resonance instrument for soil-water content measurement: sensor configurations. *Soil Sci. Soc. Am. J.* 51:287-290.

Phene, C.J., R.J. Reginato, B. Itier, and B.R. Tanner. 1990. Sensing irrigation needs. in *Management of Farm Irrigation Systems*. ed. G.J. Hoffman, T.A. Howell, K.H. Solomon. 207-252. ASAE Monograph. St. Joseph, MI: ASAE.

Pogue, W.R. 1990. Watermark soil moisture sensor - an update. In ASAE Winter Meetings. Chicago. Paper no. 90-2582. St. Joseph, MI: ASAE.

Ramo, S., J.R. Whinnery, and T. Van Duzer. 1994. *Fields and Waves in Communications Electronics*. 3rd edition. New York: John Wiley & Sons, Inc.

Rao, N.N. 1977. *Elements of Engineering Electromagnetics*. Englewood Cliffs, New Jersey: Prentice-Hall.

Rogers, H.H. and P.A. Bottomley. 1987. In situ nuclear magnetic resonance imaging of roots: influence of soil type, ferromagnetic particle content, and soil water. *Agron. J.* 79:957-965.

Roth, K., R. Schulin, H. Fluhler, and W. Attinger. 1990. Calibration of time domain reflectometry for water content measurement using a composite dielectric approach. *Water Resour. Res.* 26:2267-2273.

Selker, J.S., L.Graff, and T. Steenhuis. 1993. Non-invasive time domain reflectometry moisture measurement probe. *Soil Sci. Soc. Am. J.* 57:934-936.

Selker, J.S., 1993. Class notes on BRE 540: vadose zone instrumentation lab course. Department of Bioresource Engineering, Oregon State University.

Sheets, K.R., and J.M.H. Hendrickx. 1995. Non-invasive soil water content measurement using electromagnetic induction. In *Vadose Zone Hydrology: Cutting Across Disciplines,* ed. D. Silva, 129-130. University of CA., Davis: Kearney Foundation of Soil Science International Conference Proceedings.

Thomson, S.J., and C.F. Armstrong. 1987. Calibration of the Watermark Model 200 soil moisture sensor. *Applied Engineering in Agriculture,* 3:186-189. St. Joseph, MI: ASAE.

Tollner, E.W. and W.L. Rollwitz. 1987. Nuclear magnetic resonance for moisture analysis. In ASAE Summer Meetings, Baltimore, MD. Paper no. 87-1008. St. Joseph, MI: ASAE.

Topp, G.C., J.L. Davis and A.P. Annan. 1980. Electromagnetic determination of soil water content: measurements in coaxial transmission lines. *Water Resour. Res.* 16:574-582.

Topp, G.C., M. Yanuka, W.D. Zebchuk, and S. Zegelin., 1988. Determination of electrical conductivity using time domain reflectometry: soil and water experiments in coaxial lines. *Water Res. Res.* 24:945-952.

Topp, G.C., and W.D. Reynolds. 1992. *Advances in measurement of soil physical properties: bringing theory into practice.* SSSA Spec. Publ. 30. Madison, WI: SSSA.

Van Loon, W.K.P., E. Perfect, P.H. Groenevelt. and B.D. Kay. 1990. A new method to measure bulk electrical conductivity in soils with time domain reflectometry. *Can. J. Soil Sci.* 70:403-410.

Vinegar, H.J. 1986. X-Ray CT and NMR imaging of rocks. *Journal of Petroleum Technology* March 1986. 257-259.

Wang, D., and I. R. McCann. 1988. An evaluation of Watermark soil water content sensors for irrigation scheduling. In Pacific Northwest Region Meeting of ASAE and CSAE, Pendleton, OR. Paper no. 88-301. St. Joseph, MI: ASAE.

Zegelin, S.J., I. White and D.R. Jenkins. 1989. Improved field probes for soil water content and electrical conductivity measurement using time domain reflectometry. *Water Resour. Res.* 25:2367-2376.